Published in final edited form as:
Schizophr Res. 2012 December ; 142(1-3): 188–199. doi:10.1016/j.schres.2012.09.015.

Transcriptomic Analysis of *Postmortem* Brain identifies Dysregulated Splicing Events in Novel Candidate Genes for Schizophrenia

Ori S. Cohen[1,2], **Sarah Y. Mccoy**[1,2], **Frank A. Middleton**[2], **Sean Bialosuknia**[1,2], **Yanli Zhang-James**[2], **Lu Liu**[2], **Ming T. Tsuang**[3,4,5], **Stephen V. Faraone**[2], and **Stephen J. Glatt**[1,2,*]

[1]Psychiatric Genetic Epidemiology & Neurobiology Laboratory (PsychGENe Lab), SUNY Upstate Medical University, Syracuse, NY, U.S.A

[2]Departments of Psychiatry and Behavioral Sciences & Neuroscience and Physiology, Medical Genetics Research Center, SUNY Upstate Medical University, Syracuse, NY, U.S.A

[3]Center for Behavioral Genomics, Department of Psychiatry, University of California, San Diego, La Jolla, CA, U.S.A

[4]Harvard Institute of Psychiatric Epidemiology and Genetics, Departments of Epidemiology and Psychiatry, Harvard School of Public Health and Harvard Medical School, Boston, MA, U.S.A

[5]Veterans Affairs San Diego Healthcare System, San Diego, CA, U.S.A

Abstract

The diverse spatial and temporal expression of alternatively spliced transcript isoforms shapes neurodevelopment and plays a major role in neuronal adaptability. Although alternative splicing is extremely common in the brain, its role in mental illnesses such as schizophrenia has received little attention. To examine this relationship, *postmortem* brain tissue was obtained from 20 individuals with schizophrenia (SZ) and 20 neuropsychiatrically normal comparison subjects. Gray matter samples were extracted from two brain regions implicated in the disorder: Brodmann area 10 and caudate. Affymetrix Human Gene 1.0 ST arrays were used on four subjects per group to attain an initial profile of differential expression of transcribed elements within and across brain regions in SZ. Numerous genes of interest with altered mRNA transcripts were identified by microarray through the differential expression of particular exons and 3′ untranslated regions (**UTRs**) between diagnostic groups. Select microarray results—including dysregulation of *ENAH* exon 11a and *CPNE3* 3′UTR—were verified by qRTPCR and replicated in the remaining independent sample of 16 SZ patients and 16 normal comparison subjects. These results, if further

*To whom correspondence should be addressed: Stephen J. Glatt, Ph.D., SUNY Upstate Medical University, 750 East Adams Street, Syracuse, NY 13210, Phone: 1-(315)-464-7742, Fax: 1-(315)-464-7744, glatts@upstate.edu.

The authors report no conflicts of interest.

Ori S. Cohen designed and performed the experiments and wrote the manuscript.
Sarah Y. Mccoy, Sean Bialosuknia, Lu Liu, and Yanli Zhang-James assisted with experiments and contributed sections of text to the manuscript.
Frank A. Middleton participated in the design and execution of the neuroanatomical and molecular biological aspects of the experiments.
Ming T. Tsuang, Stephen V. Faraone, & Stephen J. Glatt designed the experiments and wrote and edited portions of the manuscript.

replicated, clearly illustrate the importance of Identifying transcriptomic variants in expression studies, and implicate novel candidate genes in the disorder.

INTRODUCTION

One method commonly employed to unravel the underlying biology of schizophrenia (**SZ**) is transcriptomic profiling of *postmortem* brain tissue (Glatt et al., 2005; Horvath et al., 2011; Mirnics et al., 2006). Most prior transcriptomic studies of the brain in SZ overlooked a potentially important source of phenotypic diversity: the expression of alternatively spliced variants (**ASV**s). Alternative splicing is a major mechanism by which eukaryotes create enormous proteomic diversity from a smaller-than-expected number of genes. The manner in which elements of a particular gene are spliced has a significant impact on protein function. In fact, the discrete ASVs of some genes have diametrically opposed physiological functions (Clark et al., 2007); thus, traditional discussions about a the function of a given gene may be moot unless a particular ASV of the gene is invoked.

Transcriptome-wide sequence analysis has detected splicing events in up to 95% of multi-exon genes (Pan et al., 2008). Alternative splicing events are tissue-specific, and can be regionally specific within a tissue, including the brain (Twine et al., 2011), resulting in an extremely complex expression profile. These diverse splicing patterns dictate important regulatory decisions in many steps of neuronal development, including axon guidance (Schmucker et al., 2000; Zipursky et al., 2006), cell-fate determination (Dho et al., 1999; Dho et al., 2006; Reugels et al., 2006), and synaptogenesis (Li et al., 2007). Notably, a small handful of candidate genes for SZ have been found to exhibit abnormal splicing patterns in individual regions of *postmortem* brain (Glatt et al., 2011), including *CTNNA2* (Mexal et al., 2008), *DISC1* (Nakata et al., 2009), *ERBB4* (Law et al., 2007), *ESR1* (Weickert et al., 2008), *GRM3* (Sartorius et al., 2008), and *NRG1* (Tan et al., 2007). It is not clear if these splicing patterns are abnormal only in those specific brain regions or if other regions are similarly affected.

The key technological advance provided by the Affymetrix Human Gene 1.0 ST arrays is measurement of the expression levels of individual exons and UTRs (hereafter collectively referred to as transcribed elements, or **TE**s). The aim of the current study was to use this technology to compare the expression profiles of TEs across the whole transcriptome in *postmortem* brain of individuals with SZ and control subjects in two brain regions previously implicated in the disorder (Brodmann Area 10 [**BA10**] and caudate head) (Ellison-Wright et al., 2008; Goghari, 2010; Yu et al., 2010) in order to identify alternative splicing abnormalities in SZ and to estimate their regional specificity.

METHODS

Samples

Postmortem brain samples were obtained from 20 SZ and 20 neuropsychiatrically normal comparison (**NC**) subjects in the Harvard Brain Tissue Resource Center. All tissues were collected with the full consent of the family or next of kin of the deceased. A "**discovery sample**" was constructed of four SZ and four NC subjects matched on age, sex, *postmortem* interval, and RNA integrity Number (**RIN**) (Table 1). The SZ discovery sample was selected to include two subjects on antipsychotic medication at the time of death and two who were not, allowing identification and exclusion of some medication effects from further validation steps (we note here that this contrast of small samples did not have adequate power to detect all medication-related effects, but it does provide one basis for filtering out genes that were strongly regulated by medication). Subsequent to verification, select observations from

microarray analysis of the discovery sample were tested for replication in an independent, larger, and less homogeneous group of SZ and NC subjects (the "**replication sample**").

RNA Extraction and Purification

Gray matter tissue samples were dissected from two brain regions (BA10 and CAUD). All brains had a pH between 6 and 7. Samples remained frozen over dry ice until placed in RLT buffer with β-mercaptoethanol and homogenized using Qiashredder columns for subsequent nucleic acid isolation using Qiagen AllPrep DNA/RNA Mini Kits (see Supplemental Methods for further details). Using a Bioanalyzer 2100 and an RNA Nanochip, purity of each sample was determined by the A260:280 ratio, with acceptable values ranging from 1.8–2.2. The quality of each sample was assured by a RIN≥6 and visual confirmation of clear, distinct 28S and 18S rRNA peaks.

Microarray Procedures

Reverse-transcription, hybridization, and scanning were performed according to well-established protocols. Ambion WT Expression Kits were used for amplification and Affymetrix WT Terminal Labeling Kits were used for labeling. Total RNA was reverse-transcribed and hybridized onto GeneChip Human Gene 1.0 ST Arrays (Affymetrix) and scanned on a GeneChip 7G/4C scanner (Affymetrix). The Human Gene 1.0ST Array improves upon previous generations of Affymetrix arrays by probing the entire length of each transcript, rather than the 3′ end only. The Gene 1.0 ST Array interrogates 28,869 well-annotated genes with 764,885 distinct probes, with an average of one probe per exon and 27 probes per transcript. The array has greater than 99 percent coverage of NM sequences present in the November 3, 2006, RefSeq database (Affymetrix, 2007).

Microarray Data Preparation

Partek Genomics Suite software was utilized for all analyses of microarray scan data. Corrections for background signal were made by robust multi-array average (**RMA**) (Irizarry et al., 2003). The set of eight GeneChips was standardized using quantile normalization, and expression levels of each probe underwent *log*-2 transformation to yield data distributions more closely approximating normality. Summarization of redundant probesets was obtained by median polish. Probesets with a signal:noise ratio of less than 3.0 were excluded from subsequent analyses (Handran et al., 2002); this led to the exclusion of six probes from the BA10 dataset and seven probes from the CAUD dataset.

Microarray Data Analyses

Primary analyses were designed to detect genes with significantly different TE expression between diagnostic groups, potentially indicating different alternative splicing events between them. SZ and NC groups were compared on mean expression levels of all TEs in each gene on a gene-by-gene basis through ANCOVAs and inspection of interaction terms, as described previously (Glatt et al., 2009; Partek Incorporated, 2008) and in more detail in the Supplemental Methods. The key term for the present analyses was the interaction of TE identity (**ID**) with diagnostic group, which allowed for the detection of differences in the expression of one or more TEs in a gene between diagnostic groups (Partek Incorporated, 2008). The significance of these interaction terms (one per gene) was judged against a stringent Bonferroni-corrected threshold of $p=2.47e^{-06}$, and post-hoc *F*-tests were used to identify the specific dysregulated TE(s) in the genes showing significant interactions.

Genes influenced by a significant interaction of diagnosis and TE ID in one or more brain regions were subjected to the DAVID algorithm (Dennis et al., 2003) to determine if the set was enriched with genes mapping to a particular biological pathway, or genes containing

particular protein domains, which might indicate that the corresponding exonic sequences shared by these genes might provide the basis for their targeting by a common alternative-splicing regulator(s).

Reverse Transcription and Quantitative PCR

Quantitative reverse transcription (**qRT**) PCR was performed to confirm and validate select microarray results. Concentrations of total RNA isolates were adjusted prior to RT, and the same amount of total RNA was used in each reaction (20 ng/ul). QuantiTect RT kits (Qiagen) were used according to the manufacturer's protocol. Each subject's cDNA was run by qRTPCR in duplicate for each primer set (Supplemental Tables). Additional details are provided in Supplemental Methods.

Expression of each dysregulated TE was evaluated and compared with a non-dysregulated TE of the same gene. The primer set amplifying the non-dysregulated region of the transcript was considered the "control" primer set. The expression value from the primer set that amplified the dysregulated region (considered the "experimental" primer set) was then compared to that of the control primer set using the $\Delta\Delta C_T$ method (Supplemental Methods). TE dysregulation was confirmed using linear regression models with diagnosis, age, sex, PMI, and RIN as independent predictors. The significance of the effect of diagnosis was determined with a 1-tailed $p<0.05$ for this term after backward removal of clearly non-significant terms ($p<0.20$) from each regression model.

RESULTS

Discovery Analyses

In BA10 from four SZ subjects and four well-matched NC subjects, 43 transcripts were influenced by a Bonferroni-corrected significant interaction of diagnosis and TE ID, indicative of differential expression of one or some (but not all) TEs between diagnostic groups (Table 2). DAVID analysis found no particular biological pathways or protein domains enriched among these 43 genes.

In CAUD, 31 results surpassed the Bonferroni-adjusted significance threshold (Table 3). These 31 transcripts were significantly enriched with genes sharing common protein domains, suggesting a possible basis for their common exonic dysregulation. The most significantly enriched protein-domain annotations were spectrin repeats ($p=5.07e^{-04}$) and actinin-type actin-binding domains ($p=6.09e^{-04}$), both of which were present in the same three transcripts. This ratio (3/31) represents an approximately 80-fold enrichment of both annotations compared to chance expectation. One biological pathway (Agrin in Postsynaptic Differentiation) was also over-represented at a Bonferroni-corrected level of significance ($p=0.019$). The appearance of two genes in this pathway on a list of 31 transcripts represents an approximately 52-fold enrichment compared to chance expectation.

CPNE3, was the lone gene whose modulation by a diagnosis-x-TE ID interaction surpassed Bonferroni-corrected significance in both brain regions; however, 340 additional transcripts were influenced by at least a nominally significant interaction of diagnosis and TE ID in both brain regions (Table 4). This list of 341 transcripts was also significantly enriched with genes with one or more common protein domains, including a 9.4-fold enrichment of genes with actinin-type actin-binding domains ($p=8.45e^{-03}$). The most significant enrichment was for genes containing one or more fibronectin type-III-like fold ($p=7.14e^{-03}$), with ten out of 341 genes containing this domain, representing a 2.9-fold enrichment beyond chance expectation. Other protein domains enriched among the genes on this list included calponin-like actin-binding (six genes; 4.6-fold enrichment; $p=9.55e^{-03}$), peptidase C1A, papain C-

terminal (three genes; 11.5-fold enrichment; $p=2.68e^{-02}$), and histone core (four genes; 5.0-fold enrichment; $p=4.50e^{-02}$). No biological pathways were enriched at a Bonferroni-corrected level of significance within the list of 341 transcripts.

Confirmation and Replication Analyses

We selected three genes for confirmation and replication analyses. First was *CPNE3*, which exhibited a Bonferroni-corrected significant interaction in both BA10 ($F=15.00$, $p=6.6e^{-24}$) and CAUD ($F=18.52$, $p=1.0e^{-27}$). As shown in Figure 1, the significant difference in expression detected between diagnostic groups by microarray in both brain regions was relegated to the most distal end of the gene's 3′UTR (**panel A:** BA10, $F=35.89$, $p=9.7e^{-4}$; **panel B**: CAUD, $F=113.56$, $p=4.0e^{-5}$), suggesting that SZ subjects expressed transcripts with relatively shorter 3′UTRs. In the same discovery sample used for the microarray analyses described above, qRTPCR confirmed differences between diagnostic groups in the expression levels of this segment of the 3′UTR of *CPNE3* relative to a control region of the gene (upstream in the 3′UTR). This difference attained statistical significance in both CAUD ($p=0.001$) and BA10 ($p=0.041$). We next sought to replicate the decreased expression level of the distal 3′UTR segment of *CPNE3* (again, relative to the non-differentially expressed proximal 3′UTR segment) in the remaining 16 SZ and 16 NC *postmortem* brain tissue samples from the Harvard Brain Tissue Resource Center. In this fully independent sample, we successfully replicated a highly significant decrease in 3′UTR expression in BA10 in SZ ($p<0.001$), and in CAUD SZ samples as well ($p=0.034$), indicating that this result generalizes across samples and brain regions.

The second gene followed-up by qRTPCR was *ENAH*, which was chosen based on the appearance of exonic dysregulation in the vicinity of a known splice site. Initial analyses of the small discovery sample by microarray showed that *ENAH* expression levels were influenced by a Bonferroni-corrected significant interaction of diagnosis and TE ID in BA10 ($F=4.98$, $p=5.5e^{-07}$) but not in CAUD ($F=0.57$, $p=0.890$). As shown in Figure 2, SZ and NC subjects had equivalent levels of TE expression in most gene regions in both BA10 (**panel A**) and CAUD (**panel B**); however, there was a significant decrease in exon 11a expression in SZ in BA10 ($F=15.96$, $p=0.007$). This precise pattern was recapitulated by qRTPCR, with a significant SZ-associated decrease in *ENAH* exon 11a expression (relative to a non-dysregulated region of the gene: the boundary of exons 2 and 3) confirmed in BA10 ($p=0.037$), and no significant difference observed in CAUD ($p=0.141$) in the discovery sample. When extending this evaluation to the replication sample, the significant dysregulation of *ENAH* exon 11a was again detected in BA10 in SZ ($p=0.035$); unexpectedly, we also detected a significant decrease in exon 11a expression in CAUD in the replication sample by qRTPCR ($p=0.001$).

The last result selected for confirmation by qRTPCR was the up-regulation of *KLHL5* exon 10 in SZ. This gene's expression levels showed highly significant evidence of a diagnosis by TE ID interaction in both BA10 ($F=4.17$; $p=1.1e^{-4}$) and CAUD ($F=3.89$; $p=2.4e^{-4}$) by microarray. Interestingly, the strongest difference in expression in both brain regions did not involve the use of the known alternate transcription start-sites in the 5′ end of the gene, but was found at exon 10 (BA10: $F=5.96$, $p=0.050$; CAUD: $F=8.79$ $p=0.025$), where SZ subjects exhibited higher expression on average than NC subjects. Reanalysis of the discovery samples by qRTPCR did not directly verify the microarray results, as expression levels of the exon 10 and 11 boundary (relative to a non-dysregulated region of the gene: the boundary of exons 6 and 7) were not significantly higher in SZ (BA10: $p=0.229$; CAUD: $p=1.000$). Yet, when we examined the expression levels of this exon by qRTPCR in the independent replication sample, we again observed a significant increase in exon 10 expression in SZ in BA10 ($p=0.011$), though not in CAUD ($p=1.000$). Our inability to

consistently verify the precise results observed by microarray in the discovery sample nor confirm them in the replication sample is perhaps not surprising given the relatively lax criteria used in selecting this gene for follow-up study relative to the Bonferroni-corrected significant results that drove our follow-up work on *CPNE3* and *ENAH*. However, further investigation of *KLHL5's* transcriptomic profile by direct sequencing or qRTPCR using primers with greater coverage may resolve this uncertainty in the future.

DISCUSSION

The main objective of this study was to assess how common and widespread exonic expression abnormalities are in *postmortem* brain in SZ. Our work suggests they are not uncommon, and are more complex than initially conceived, involving not only alternative splicing of traditional cassette exons, but also selection of mutually exclusive exons, alternate promoter selection, and 3′UTR constitution. By comparing brain regions linked to the disorder, as well as medicated and unmedicated patients (although in just a small, initial discovery sample), we were able to identify some expression abnormalities that generalized across regions and which may reflect stable traits associated with the disorder. Further work could evaluate whether such expression abnormalities arise from inherited mutations or biological insults acquired early in development. In contrast, most TE expression abnormalities observed in this study were restricted to either BA10 or CAUD. Such regionally specific abnormalities may be less likely attributable to regulatory effects of "splicing quantitative trait loci" (sQTLs) than are ubiquitous expression abnormalities; however, this does not preclude the possibility that sQTLs could be differentially regulated in different cells or brain regions. Such region-specific effects might reflect the diverse developmental influences governing maturation of those brain regions, or their differential sensitivity to schizophrenogenic environmental insults. Alternatively, these region-specific effects may result from differential expression of facilitators or inhibitors of splicing (*i.e.,* alternative splicing regulators) in a similarly region-specific manner. In support of this possibility, we found nominally significant evidence of dysregulation of full-length splicing-regulatory transcripts such as *HNRNPH1* (p=0.004), *HNRNPH3* (p=0.039), *HNRNPC* (p=0.040), and *SFRS16* (p=0.018) in BA10 but not CAUD in the same samples examined here (unpublished data). The systematic follow-up of our results and evaluation of these contributory possibilities should be a high priority for future work.

Our analyses of microarray-derived TE expression data from a small sample of well-matched SZ and NC samples generated many leads, two of which we validated (either perfectly or partially) using another, more sensitive analytic technique (qRTPCR). These two results also replicated in a larger, more heterogeneous, and fully independent sample of SZ and NC subjects. One of these genes (*CPNE3*, a calcium-dependent membrane-binding protein that co-localizes with phosphorylated focal adhesion kinase at the leading edge of migrating cells (Heinrich et al., 2010)) has never before been implicated in SZ, and the other (*ENAH*, an actin-associated protein involved in cytoskeleton remodeling and neuronal projection) was targeted just once among a panel of 18 target genes (Kahler et al., 2008), highlighting the advantage of a transcriptome-wide approach that can generate new candidate genes and hypotheses regarding this complex multifactorial disorder.

Aside from generating new hypotheses, this work validates our prior blood-based biomarker study of TE expression in SZ (Glatt et al., 2009). For example, 44 (28%) of the 156 genes that we previously found to exhibit Bonferroni-corrected significant abnormal expression of a TE in peripheral blood cells in psychotic subjects (SZ plus psychotic bipolar disorder) were also found to have at least nominally significant abnormal TE expression in either BA10 or CAUD in the present study of *postmortem* brain. Further, eight of those 156 genes (*ADAR*, *ARHGAP26*, *BIRC6*, *MAPK14*, *STXBP2*, *SYNE2*, *UTRN*, and *ZDHHC17*) had

TEs that were Bonferroni-corrected significant in blood and at least nominally significantly dysregulated in both brain regions, a result very unlikely to occur by chance (binomial test, $p<0.0001$). This type of convergence suggests two areas for future work; the pursuit of factors that may be capable of disrupting the expression of particular TEs regardless of tissue type, and the validation of blood-based biomarkers for these disorders.

This study also lends support to hypotheses generated by the prior work of others. In particular, the dysregulation of *ERBB4* exons we observed in both BA10 and CAUD confirmed prior *postmortem* work linking particular splice variants of this neuregulin-1 cofactor to risk for the disorder (Kao et al., 2010; Law et al., 2007; Silberberg et al., 2006). We could not confirm in our small microarray sample the differential splicing of other previously observed results for SZ candidate genes, such as *CTNNA2*, *DISC1*, *ESR1*, *GRM3*, and *NRG1*; however, because our microarray sample was very small it is possible that these effects may have eluded detection in our sample due primarily to lack of power. This seems particularly likely for *DISC1* and *NRG1*, as we did observe patterns of TE-expression data suggestive of differential splicing of known alternatively spliced TEs of these genes that did not attain statistical significance due to relatively large variance. It is also possible that the prior results are specific for regions of the brain (*e.g.,* BA9) we did not have available for analysis. Yet, several other genes for which functionally distinct and neurodevelopmentally important splice variants are known (including *NUMBL*, *DSCAM*, *FGF*, *SNAP25*, and Neuroligins 2 and 4X) were also found in our study to have SZ-associated dysregulation of one or more exons in *postmortem* BA10, but not CAUD, reinforcing the importance of pursuing both ubiquitous and regionally specific alterations in exonic expression.

This study, like all human *postmortem* studies of brain disorders, is subject to several limitations. Primarily, because *postmortem* brain tissue from schizophrenia patients is an extremely rare and highly prized commodity, the sample size available for this study was quite small. Our design, which included carving both discovery and replication samples from the same small primary sample, further exacerbated this problem; however, this approach was taken to foster more confidence in those results that did survive replication. This anonymized sample was also not ideal because we were unable to determine the ancestry of each subject, which might relate to either genetically or environmentally mediated differences in TE expression. Thus, if the SZ and NC groups differed systematically in ancestry and if the represented ancestral groups differed systematically in expression levels of particular mRNA isoforms, then it is possible we would have falsely attributed some of these ancestry-related differences to diagnosis. Another limitation is that, because we did not have access to brain tissue from first-episode or prodromal patients, we are unable to rule out the possibility that the observed results are a function of (rather than cause of or contributor to) having SZ, such as treatment, hospitalization, medical and psychiatric comorbidity, and substance use disorders, all of which are more common among SZ patients than NC subjects. In an attempt to control for these factors, we followed-up by qRTPCR only those genes that did not differ in TE expression between the treated and untreated subgroups; however, power to detect such differences was quite low due to the small number of subjects in each group and the fact that all patients had been medicated at some time, even if not at the time of death. Future *in vitro* studies will be instrumental for validating these splicing abnormalities and more strongly attributing them to sequence variation rather than personal, clinical, agonal, or other factors.

In conclusion, we demonstrated the utility of examining the functional genomic output of the human brain in SZ using TE- and brain-region-specific profiling of expression intensity by microarray. The SZ-associated TE-expression abnormalities validated and replicated in this study would not have been detected using earlier generations of “whole-transcript”

expression arrays. Looking back, this might explain in part why prior microarray-based studies of *postmortem* brain tissue in SZ have not routinely observed identical patterns of transcript dysregulation. Looking ahead, the use of RNA sequencing should facilitate the detection of additional subtle splicing (and other RNA-processing) variations that might characterize particular brain regions (or the whole organism) in SZ. Additional work is needed to extend our results into other samples and other implicated brain regions, as well as to uncover the factors (genetic or otherwise) that influence the observed expression abnormalities in brain and in blood. Ultimately the generation of region-specific transcriptome profiles that include information on the relative abundance of each splice variant may prove essential for gaining a better understanding of the biological basis of SZ and the development of better biomarkers and treatments for the disorder.

Supplementary Material

Refer to Web version on PubMed Central for supplementary material.

Acknowledgments

This work was supported in part by grants R21MH075027 (M.T.T.), P50MH081755-0003 (S.J.G.), and R01MH085521 (S.J.G.) from the U.S. National Institutes of Health, a Young Investigator Award and the Sidney R. Baer, Jr. Prize for Schizophrenia Research (S.J.G.) from NARSAD: The Brain and Behavior Research Fund, and A Research Grant from The Gerber Foundation (S.J.G.). The authors wish to thank Dr. Francine M. Benes, George Tejada, and the staff of the Harvard Brain Tissue Resource Center for providing *postmortem* brain tissue samples, Dr. George H. Trksak for determining medication status at the time of death of the SZ patients, and those subjects and family members who made this study possible.

The funding source had no role in designing the study, analyzing the data, or interpreting the results.

References

Affymetrix, Inc. Data Sheet: GeneChip® Gene 1.0 ST Array System for Human, Mouse and Rat. 2007.

Clark TA, Schweitzer AC, Chen TX, Staples MK, Lu G, Wang H, Williams A, Blume JE. Discovery of tissue-specific exons using comprehensive human exon microarrays. Genome Biology. 2007; 8(4):R64. [PubMed: 17456239]

Dennis G Jr, Sherman BT, Hosack DA, Yang J, Gao W, Lane HC, Lempicki RA. DAVID: Database for Annotation, Visualization, and Integrated Discovery. Genome Biology. 2003; 4(5):3.

Dho SE, French MB, Woods SA, McGlade CJ. Characterization of four mammalian numb protein isoforms. Identification of cytoplasmic and membrane-associated variants of the phosphotyrosine binding domain. Journal of Biological Chemistry. 1999; 274(46):33097–33104. [PubMed: 10551880]

Dho SE, Trejo J, Siderovski DP, McGlade CJ. Dynamic regulation of mammalian numb by G protein-coupled receptors and protein kinase C activation: Structural determinants of numb association with the cortical membrane. Molecular Biology of the Cell. 2006; 17(9):4142–4155. [PubMed: 16837553]

Ellison-Wright I, Glahn DC, Laird AR, Thelen SM, Bullmore E. The anatomy of first-episode and chronic schizophrenia: an anatomical likelihood estimation meta-analysis. Am J Psychiatry. 2008; 165(8):1015–1023. [PubMed: 18381902]

Glatt SJ, Chandler SD, Bousman CA, Chana G, Lucero GR, Tatro E, May T, Lohr JB, Kremen WS, Everall IP, Tsuang MT. Alternatively Spliced Genes as Biomarkers for Schizophrenia, Bipolar Disorder and Psychosis: A Blood-Based Spliceome-Profiling Exploratory Study. Curr Pharmacogenomics Person Med. 2009; 7(3):164–188. [PubMed: 21532980]

Glatt SJ, Cohen OS, Faraone SV, Tsuang MT. Dysfunctional gene splicing as a potential contributor to neuropsychiatric disorders. Am J Med Genet B Neuropsychiatr Genet. 2011; 156B(4):382–392. [PubMed: 21438146]

Glatt SJ, Everall IP, Kremen WS, Corbeil J, Sasik R, Khanlou N, Han M, Liew CC, Tsuang MT. Comparative gene expression analysis of blood and brain provides concurrent validation of SELENBP1 up-regulation in schizophrenia. Proceedings of the National Academy of Sciences of the United States of America. 2005; 102(43):15533–15538. [PubMed: 16223876]

Goghari VM. Executive functioning-related brain abnormalities associated with the genetic liability for schizophrenia: an activation likelihood estimation meta-analysis. Psychol Med. 2010:1–14. [PubMed: 20942994]

Handran, S.; Pickett, S.; Verdick, D. Key Considerations for Accurate Microarray Scanning and Image Analysis. In: Kamberova, G.; Shah, S., editors. DNA Array Image Analysis: Nuts & Bolts. DNA Press, LLC; Salem, MA: 2002. p. 83-98.

Heinrich C, Keller C, Boulay A, Vecchi M, Bianchi M, Sack R, Lienhard S, Duss S, Hofsteenge J, Hynes NE. Copine-III interacts with ErbB2 and promotes tumor cell migration. Oncogene. 2010; 29(11):1598–1610. [PubMed: 20010870]

Horvath S, Janka Z, Mirnics K. Analyzing schizophrenia by DNA microarrays. Biol Psychiatry. 2011; 69(2):157–162. [PubMed: 20801428]

Irizarry RA, Hobbs B, Collin F, Beazer-Barclay YD, Antonellis KJ, Scherf U, Speed TP. Exploration, normalization, and summaries of high density oligonucleotide array probe level data. Biostatistics. 2003; 4(2):249–264. [PubMed: 12925520]

Kahler AK, Djurovic S, Kulle B, Jonsson EG, Agartz I, Hall H, Opjordsmoen S, Jakobsen KD, Hansen T, Melle I, Werge T, Steen VM, Andreassen OA. Association analysis of schizophrenia on 18 genes involved in neuronal migration: MDGA1 as a new susceptibility gene. Am J Med Genet B Neuropsychiatr Genet. 2008; 147B(7):1089–1100. [PubMed: 18384059]

Kao WT, Wang Y, Kleinman JE, Lipska BK, Hyde TM, Weinberger DR, Law AJ. Common genetic variation in Neuregulin 3 (NRG3) influences risk for schizophrenia and impacts NRG3 expression in human brain. Proc Natl Acad Sci U S A. 2010; 107(35):15619–15624. [PubMed: 20713722]

Law AJ, Kleinman JE, Weinberger DR, Weickert CS. Disease-associated intronic variants in the ErbB4 gene are related to altered ErbB4 splice-variant expression in the brain in schizophrenia. Human Molecular Genetics. 2007; 16(2):129–141. [PubMed: 17164265]

Li Q, Lee JA, Black DL. Neuronal regulation of alternative pre-mRNA splicing. Nature Reviews Neuroscience. 2007; 8(11):819–831.

Mexal S, Berger R, Pearce L, Barton A, Logel J, Adams CE, Ross RG, Freedman R, Leonard S. Regulation of a novel alphaN-catenin splice variant in schizophrenic smokers. American Journal of Medical Genetics B Neuropsychiatric Genetics. 2008; 147B(6):759–768.

Mirnics K, Levitt P, Lewis DA. Critical appraisal of DNA microarrays in psychiatric genomics. Biol Psychiatry. 2006; 60(2):163–176. [PubMed: 16616896]

Nakata K, Lipska BK, Hyde TM, Ye T, Newburn EN, Morita Y, Vakkalanka R, Barenboim M, Sei Y, Weinberger DR, Kleinman JE. DISC1 splice variants are upregulated in schizophrenia and associated with risk polymorphisms. Proceedings of the National Academy of Sciences of the United States of America. 2009; 106(37):15873–15878. [PubMed: 19805229]

Pan Q, Shai O, Lee LJ, Frey BJ, Blencowe BJ. Deep surveying of alternative splicing complexity in the human transcriptome by high-throughput sequencing. Nat Genet. 2008; 40(12):1413–1415. [PubMed: 18978789]

Partek Incorporated. Partek Documentation. Partek Incorporated; 2008.

Reugels AM, Boggetti B, Scheer N, Campos-Ortega JA. Asymmetric localization of Numb:EGFP in dividing neuroepithelial cells during neurulation in Danio rerio. Developmental Dynamics. 2006; 235(4):934–948. [PubMed: 16493689]

Sartorius LJ, Weinberger DR, Hyde TM, Harrison PJ, Kleinman JE, Lipska BK. Expression of a GRM3 splice variant is increased in the dorsolateral prefrontal cortex of individuals carrying a schizophrenia risk SNP. Neuropsychopharmacology. 2008; 33(11):2626–2634. [PubMed: 18256595]

Schmucker D, Clemens JC, Shu H, Worby CA, Xiao J, Muda M, Dixon JE, Zipursky SL. Drosophila Dscam is an axon guidance receptor exhibiting extraordinary molecular diversity. Cell. 2000; 101(6):671–684. [PubMed: 10892653]

Silberberg G, Darvasi A, Pinkas-Kramarski R, Navon R. The involvement of ErbB4 with schizophrenia: association and expression studies. American Journal of Medical Genetics B Neuropsychiatric Genetics. 2006; 141B(2):142–148.

Tan W, Wang Y, Gold B, Chen J, Dean M, Harrison PJ, Weinberger DR, Law AJ. Molecular cloning of a brain-specific, developmentally regulated neuregulin 1 (NRG1) isoform and identification of a functional promoter variant associated with schizophrenia. Journal of Biological Chemistry. 2007; 282(33):24343–24351. [PubMed: 17565985]

Twine NA, Janitz K, Wilkins MR, Janitz M. Whole transcriptome sequencing reveals gene expression and splicing differences in brain regions affected by Alzheimer's disease. PLoS One. 2011; 6(1):e16266. [PubMed: 21283692]

Weickert CS, Miranda-Angulo AL, Wong J, Perlman WR, Ward SE, Radhakrishna V, Straub RE, Weinberger DR, Kleinman JE. Variants in the estrogen receptor alpha gene and its mRNA contribute to risk for schizophrenia. Human Molecular Genetics. 2008; 17(15):2293–2309. [PubMed: 18424448]

Yu K, Cheung C, Leung M, Li Q, Chua S, McAlonan G. Are Bipolar Disorder and Schizophrenia Neuroanatomically Distinct? An Anatomical Likelihood Meta-analysis. Front Hum Neurosci. 2010; 4:189. [PubMed: 21103008]

Zipursky SL, Wojtowicz WM, Hattori D. Got diversity? Wiring the fly brain with Dscam. Trends in Biochemical Science. 2006; 31(10):581–588.

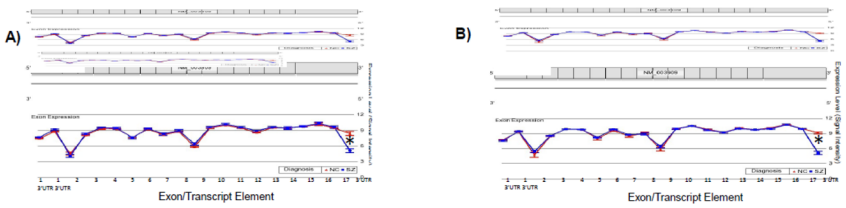

Figure 1. Exonic Expression and Alternative 3′UTR Usage of *CPNE3*in: A) BA10; and B) CAUD

Microarray results of differential probe expression of Copine3 (*CPNE3*) in Brodman Area 10 (**A**) and Caudate (**B**) in postmortem brain tissue samples from normal control subjects (NC) (n=4) and individuals with schizophrenia (SZ) (n=4). The interaction of diagnosis and exon ID was highly significant in both brain regions; in fact, it was the only gene for which a Bonferroni-corrected threshold for significance of this term was met. *There was a statistically significant difference in probe-level expression between diagnostic groups at the most distal end of the 3′UTR in both BA10 (p=9.7e-4) and CAUD (p=4.0e-5), indicating that a truncated transcript may be expressed in SZ patients.

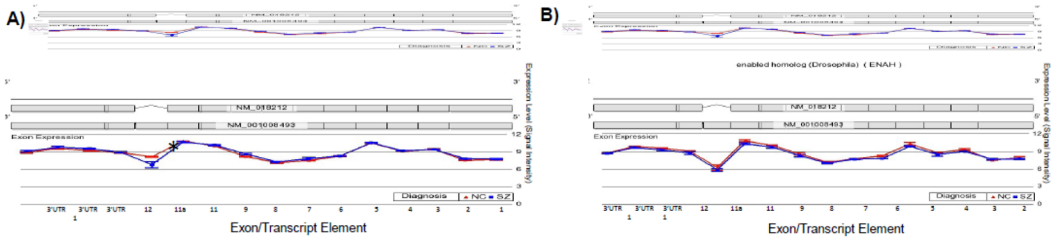

Figure 2. Exonic Expression and Alternative Splicing of *ENAH* in: A) BA10; and B) CAUD

Microarray results of differential exon expression of Enabled Homolog (*ENAH*) in Brodman Area 10 (**A**) and Caudate (**B**) in postmortem brain tissue samples from normal control subjects (NC) (n=4) and individuals with schizophrenia (SZ) (n=4). The interaction of diagnosis and exon ID was significant only in BA10, not CAUD, indicating the possibility of regionally specific differential splice-variant expression between the groups. *There was a statistically significant difference in expression between diagnostic groups at exon 11a in BA10 (p=0.047) but not CAUD (p=0.489), indicating increased expression of the short (11a) isoform in SZ patients in BA10 only.

Table 1

Demographic and Agonal Characteristics of the SZ and NC Discovery and Replication Samples

	Discovery Samples		Replication Samples	
	SZ	**NC**	**SZ**	**NC**
Sample Size: *n*	4	4	16	16
Sex: % male (*n*)	100 (4)	100 (4)	37.5 (6)	31.2 (5)
Age: mean years±S.D.	59.0±3.7	58.3±2.1	68.2±22.7	66.5±20.7
Postmortem Interval: mean hours±S.D.	24.9±4.1	24.0±3.5	18.8±7.0	21.9±5.3
RNA Integrity Number (RIN): mean±S.D.	8.0±1.2	7.8±1.3	7.9±0.5	8.3±1.3

No significant differences on any factor were observed between the SZ and NC discovery samples (all $p>0.737$) or between the SZ and NC replication samples (all $p>0.183$).

Schizophr Res. Author manuscript; available in PMC 2013 December 01.

Table 2

Transcripts Exhibiting a Bonferroni-Corrected Significant Interaction of Diagnosis (SZ *vs.* NC) and Transcript Element ID in Brodmann Area 10 (BA10)

Gene Symbol	Gene Product	Reference Sequence	Transcript Cluster ID	Probe Sets (*n*)	*F*	*p*	Direction of Dysregulation[#]
CPNE3	Copine III	NM_003909	8147172	21	15.003	$6.6e^{-24}$	↓
SCIN	Scinderin	NM_001112706	8131550	22	6.992	$5.4e^{-13}$	↑
SAMHD1	SAM domain and HD domain 1	NM_015474	8066117	18	8.354	$7.6e^{-13}$	↑
C4A	Complement component 4A (Rodgers blood group)	NM_007293	8118409	42	3.830	$2.9e^{-11}$	↑
IARS	Isoleucyl-tRNA synthetase	NM_013417	8162313	38	4.012	$5.0e^{-11}$	↑
CHI3L1	Chitinase 3-like 1 (cartilage glycoprotein-39)	NM_001276	7923547	14	9.026	$5.7e^{-11}$	↑
LPPR4	Plasticity related gene 1	NM_014839	7903214	12	9.775	$3.3e^{-10}$	↑
C4A	Complement component 4A (Rodgers blood group)	NM_007293	8118455	42	3.458	$9.8e^{-10}$	↑
SERPINA3	Serpin peptidase inhibitor, clade A (alpha-1 antiprotein)	NM_001085	7976496	9	12.930	$1.0e^{-9}$	↑
C4A	Complement component 4A (Rodgers blood group)	NM_007293	8179399	40	3.507	$1.5e^{-9}$	↑
ALOX5	Arachidonate 5-lipoxygenase	NM_000698	7927215	15	7.011	$2.6e^{-9}$	↑
CSDE1	Cold shock domain containing E1, RNA-binding	NM_001007553	7918825	21	5.214	$3.5e^{-9}$	↑
PPP3CA	Protein phosphatase 3 (formerly 2B), catalytic subunit, a	NM_000944	8101971	18	5.734	$6.3e^{-9}$	↑
TLN1	Talin 1	NM_006289	8161056	57	2.791	$6.7e^{-9}$	↑
IFI16	Interferon, gamma-inducible protein 16	NM_005531	7906400	16	6.209	$9.3e^{-9}$	↑
RNASET2	Ribonuclease T2	NM_003730	8130768	14	6.923	$1.1e^{-8}$	↑
ALDH2	Aldehyde dehydrogenase 2 family (mitochondrial)	NM_000690	7958784	15	6.330	$1.9e^{-8}$	↓
CD86	CD86 molecule	NM_175862	8082035	10	9.325	$2.2e^{-8}$	↑
CUX1	Cut-like homeobox 1	NM_181552	8135114	34	3.424	$4.5e^{-8}$	↑
MAGI2	Membrane associated guanylate kinase, WW and PDZ domain containing 2	NM_012301	8140504	25	4.003	$9.1e^{-8}$	↑
LAT2	Linker for activation of T cells family, member 2	NM_032464	8133442	16	5.454	$1.1e^{-7}$	↑
CFDP1	Craniofacial development protein 1	NM_006324	8002865	12	6.858	$1.5e^{-7}$	↓
RAB8B	RAB8B, member RAS oncogene family	NM_016530	7984112	11	7.240	$2.3e^{-7}$	↑
ERCC5	Excision repair cross-complementing 5	NM_000123	7969935	19	4.556	$2.8e^{-7}$	↑
MYO5A	Myosin VA (heavy chain 12, myoxin)	NM_000259	7988921	41	2.895	$2.9e^{-7}$	↑
PTPRC	Protein tyrosine phosphatase, receptor type, C	NM_002838	7908553	37	3.042	$3.0e^{-7}$	↑

Gene Symbol	Gene Product	Reference Sequence	Transcript Cluster ID	Probe Sets (*n*)	*F*	*p*	Direction of Dysregulation[#]
C5orf15	Chromosome 5 open reading frame 15	NM_020199	8114138	6	14.126	$3.9e^{-7}$	↑
LPCAT2	Lysophosphatidylcholine acyltransferase 2	NM_017839	7995697	14	5.525	$5.4e^{-7}$	↑
ENAH	Enabled homolog (Drosophila)	NM_001008493	7924619	16	4.976	$5.5e^{-7}$	↓
LAPTM5	Lysosomal protein transmembrane 5	NM_006762	7914270	11	6.802	$5.6e^{-7}$	↑
UHRF2	Ubiquitin-like with PHD and ring finger domains 2	NM_152896	8154316	16	4.970	$5.6e^{-7}$	↑
VTI1A	Vesicle transport through interaction with t-SNAREs homolog	NM_145206	7930524	8	9.380	$6.0e^{-7}$	↑
RAPGEF4	Rap guanine nucleotide exchange factor (GEF) 4	NM_007023	8046428	32	3.159	$7.5e^{-7}$	↓
LGALS9C	Lectin, galactoside-binding, soluble, 9C	NM_001040078	8005458	12	6.102	$8.6e^{-7}$	↑
CPVL	Carboxypeptidase, vitellogenic-like	NM_019029	8138805	16	4.779	$1.1e^{-6}$	↑
RBM33	RNA binding motif protein 33	NM_053043	8137558	7	10.236	$1.3e^{-6}$	↓
FCER1G	Fc fragment of IgE, high affinity I, receptor for; gamma	NM_004106	7906720	7	9.985	$1.7e^{-6}$	↑
ZMYND8	Zinc finger, MYND-type containing 8	NM_183047	8066786	31	3.091	$1.8e^{-6}$	↑
SAMSN1	SAM domain, SH3 domain and nuclear localization signals 1	NM_022136	8069541	11	6.252	$1.8e^{-6}$	↑
DOCK8	Dedicator of cytokinesis 8	NM_203447	8153959	52	2.422	$2.0e^{-6}$	↑
MUM1	Melanoma associated antigen (mutated) 1	NR_024247	8024255	17	4.409	$2.0e^{-6}$	↑
IGSF6	Immunoglobulin superfamily, member 6	NM_005849	8000184	7	9.837	$2.0e^{-6}$	↑
ITGB2	Integrin, beta 2 (complement component 3 receptor 3 and 4)	NM_000211	8070826	20	3.943	$2.1e^{-6}$	↑

[*] Rows are sorted by *p*-value in ascending order.

[#] of the single most differentially expressed transcribed element per gene.

Table 3

Transcripts Exhibiting a Bonferroni-Corrected Significant Interaction of Diagnosis (SZ *vs.* NC) and Transcript Element ID in Caudate Head (CAUD)

Gene Symbol	Gene Product	Reference Sequence	Transcript Cluster ID	Probe Sets (*n*)	*F*	*p**	Direction of Dysregulation#
CPNE3	Copine III	NM_003909	8147172	21	18.518	$1.0e^{-27}$	↓
UTRN[a]	Utrophin	NM_007124	8122464	72	4.946	$7.1e^{-26}$	↑
RXFP2	Relaxin	NM_130806	7968389	21	8.816	$1.6e^{-15}$	↑
DMD[a]	Dystrophin	NM_000109	8171921	95	2.540	$2.0e^{-11}$	↓
GPR98	G protein-coupled receptor 98	NM_032119	8106827	91	2.409	$6.6e^{-10}$	↓
RGPD6	Ranbp2-like and grip domain containing 6	NM_001123363	8044304	28	4.286	$2.8e^{-9}$	↓
CIT	Citron (rho-interacting, serine)	NM_007174	7966878	50	3.008	$4.6e^{-9}$	↓
SYNE1[a]	Spectrin repeat containing, nuclear envelope 1	NM_182961	8130211	158	1.873	$1.3e^{-8}$	↑
C6orf174	Chromosome 6 open reading frame 174	NM_001012279	8129392	17	5.689	$1.9e^{-8}$	↑
Unknown	Unknown	Unknown	8054557	22	4.447	$5.8e^{-8}$	↑
NME7	Non-metastatic cells 7	NM_013330	7922137	14	6.201	$8.0e^{-8}$	↑
CEP192	Centrosomal protein 192Kda	NM_032142	8020267	40	3.050	$9.7e^{-8}$	↑
KIAA0319L	KIAA0319-Like	NM_024874	7914809	24	4.042	$1.3e^{-7}$	↓
DGKI	Diacylglycerol kinase, iota	NM_004717	8143154	33	3.333	$1.4e^{-7}$	↑
KCNK2	Potassium channel, subfamily k, member 2	NM_001017425	7909730	14	5.970	$1.5e^{-7}$	↑
MYT1L	Myelin transcription factor 1-like	NM_015025	8050031	28	3.585	$2.3e^{-7}$	↑
SEC31A	Sec31 Homolog A (*S. Cerevisiae*)	NM_014933	8101376	34	3.193	$2.7e^{-7}$	↑
HSPA4	Heat shock 70kda protein 4	NM_002154	8108015	24	3.849	$3.7e^{-7}$	↑
SLC4A1AP	solute carrier family 4 (anion exchanger), member 1, adaptor protein	NM_018158	8041015	11	6.701	$6.9e^{-7}$	↓
EPB49	Erythrocyte membrane protein band 4.9 (dematin)	NM_001978	8145005	21	4.022	$8.3e^{-7}$	↓
STXBP2	Syntaxin binding protein 2	NM_006949	8025255	22	3.902	$8.4e^{-7}$	↑
RABEP1	Rabaptin, rab gtpase binding effector protein 1	NM_004703	8004111	21	4.011	$8.8e^{-7}$	↓
FBXO44	F-box protein 44	NM_001014765	7897714	13	5.689	$8.9e^{-7}$	↑
EPRS	Glutamyl-prolyl-trna synthetase	NM_004446	7924351	34	3.021	$1.0e^{-6}$	↑
C17orf44	Chromosome 17 open reading frame 44	NR_026951	8012416	6	12.700	$1.1e^{-6}$	↓
PSMA5	Proteasome (prosome, macropain) subunit, alpha type, 5	NM_002790	7918345	13	5.622	$1.1e^{-6}$	↓

Gene Symbol	Gene Product	Reference Sequence	Transcript Cluster ID	Probe Sets (*n*)	*F*	*p**	Direction of Dysregulation#
PSD3	Pleckstrin and sec7 domain containing 3	NM_015310	8149555	18	4.342	$1.3e^{-6}$	↑
TNKS2	TRF1-interacting ankyrin-related ADP-ribose polymerase 2	NM_025235	7929168	32	3.078	$1.4e^{-6}$	↑
ADORA3	Adenosine a3 receptor	NM_020683	7918533	14	5.180	$1.5e^{-6}$	↑
VWA3A	Von Willebrand factor a domain containing 3a	NM_173615	7993898	36	2.837	$2.2e^{-6}$	↓
OVOS	Ovostatin	BX647938	7961026	4	22.882	$2.3e^{-6}$	↓

* Rows are sorted by *p*-value in ascending order.

\# of the single most differentially expressed transcribed element per gene.

[a] Genes encoding proteins with actinin-type actin-binding domains.

Table 4

Transcripts Exhibiting a Significant Interaction of Diagnosis (SZ *vs.* NC) and Transcript Element ID in both Brodmann Area 10 (BA10) and Caudate (CAUD)

Gene Symbol	Gene Product	Reference Sequence	Transcript Cluster ID	Probe Sets (*n*)	BA10		CAUD	
					F	*p**	*F*	*p**
CPNE3	Copine III	NM_003909	8147172	21	15.003	$6.60e^{-24}$	18.518	$1.00e^{-27}$
CEP192	Centrosomal protein 192kDa	NM_032142	8020267	40	2.587	$6.20e^{-06}$	3.050	$9.70e^{-08}$
SCIN	Scinderin	NM_001112706	8131550	22	6.992	$5.40e^{-13}$	3.055	$5.80e^{-05}$
OVOS	Ovostatin	BX647938	7953873	4	12.265	$1.30e^{-04}$	17.412	$1.50e^{-05}$
NCKAP1L	NCK-associated protein 1-like	NM_005337	7955908	34	2.359	$1.50e^{-04}$	2.642	$1.80e^{-05}$
LCP1[a,c]	Lymphocyte cytosolic protein 1 (L-plastin)	NM_002298	7971461	20	3.062	$1.20e^{-04}$	3.169	$7.20e^{-05}$
OVOS	Ovostatin	BX647938	7961026	4	11.274	$2.10e^{-04}$	22.882	$2.30e^{-06}$
KLHL5	Kelch-like 5 (*Drosophila*)	NM_015990	8094625	12	4.170	$1.10e^{-04}$	3.891	$2.40e^{-04}$
NME7	Non-metastatic cells 7, protein expressed in (nucleoside)	NM_013330	7922137	14	3.348	$4.30e^{-04}$	6.201	$8.00e^{-08}$
LAPTM5	Lysosomal protein transmembrane 5	NM_006762	7914270	11	6.802	$5.60e^{-07}$	3.864	$4.50e^{-04}$
LAT2	Linker for activation of T cells family, member 2	NM_032464	8133442	16	5.454	$1.10e^{-07}$	3.064	$5.10e^{-04}$
ST6GAL1	ST6 beta-galactosamide alpha-2,6-sialyltranferase 1	NM_173216	8084717	8	4.984	$3.60e^{-04}$	5.319	$2.10e^{-04}$
APOC2	Apolipoprotein C-II	NM_000483	8029551	8	6.543	$3.00e^{-05}$	4.739	$5.40e^{-04}$
RPL13A	Ribosomal protein L13a	NM_012423	8030351	8	4.700	$5.80e^{-04}$	7.204	$1.10e^{-05}$
HSD17B4	Hydroxysteroid (17-beta) dehydrogenase 4	NM_000414	8107532	21	2.677	$5.10e^{-04}$	2.917	$1.60e^{-04}$
RHOV	Ras homolog gene family, member V	NM_133639	7987574	9	5.332	$8.20e^{-05}$	4.281	$6.10e^{-04}$
NACA	Nascent polypeptide-associated complex alpha subunit	NM_001113201	7964262	8	4.838	$4.60e^{-04}$	5.239	$2.40e^{-04}$
SMOX	Spermine oxidase	NM_175839	8060745	12	4.805	$2.10e^{-05}$	3.504	$6.80e^{-04}$
APOL1	Apolipoprotein L, 1	NM_145343	8072735	8	7.687	$5.80e^{-06}$	4.299	$1.20e^{-03}$
EFNA5	Ephrin-A5	NM_001962	8113433	9	6.592	$8.80e^{-06}$	3.951	$1.20e^{-03}$
JTB	Jumping translocation breakpoint	NM_006694	7920409	12	4.304	$7.90e^{-05}$	3.326	$1.10e^{-03}$
ADORA3	Adenosine A3 receptor	NM_020683	7918533	14	3.019	$1.20e^{-03}$	5.180	$1.50e^{-06}$
LEPR[b]	Leptin receptor	NM_002303	7902074	27	2.369	$6.10e^{-04}$	2.347	$6.90e^{-04}$
CPVL	Carboxypeptidase, vitellogenic-like	NM_019029	8138805	16	4.779	$1.10e^{-06}$	2.805	$1.30e^{-03}$

Gene Symbol	Gene Product	Reference Sequence	Transcript Cluster ID	Probe Sets (*n*)	BA10		CAUD	
					F	*p**	*F*	*p**
RNASET2	Ribonuclease T2	NM_003730	8130768	14	6.923	$1.10e^{-08}$	2.985	$1.40e^{-03}$
Unknown	Unknown	Unknown	8179731	17	2.967	$5.10e^{-04}$	2.800	$9.80e^{-04}$
NDUFS1	NADH dehydrogenase (ubiquinone) Fe-S protein 1, 75kDa (Na^+)	NM_005006	8058428	21	2.448	$1.50e^{-03}$	2.963	$1.30e^{-04}$
ALDH3A2	Aldehyde dehydrogenase 3 family, member A2	NM_001031806	8005638	16	2.760	$1.50e^{-03}$	3.459	$1.20e^{-04}$
HLA-E	Major histocompatibility complex, class I, E	NM_005516	8117890	9	4.056	$9.50e^{-04}$	4.130	$8.20e^{-04}$
TBXAS1	Thromboxane A synthase 1 (platelet)	NM_001130966	8136557	18	3.700	$1.80e^{-05}$	2.567	$1.90e^{-03}$
DNAJC11	DnaJ (Hsp40) homolog, subfamily C, member 11	NM_018198	7912112	20	2.614	$9.00e^{-04}$	2.567	$1.10e^{-03}$
DDRGK1	DDRGK domain containing 1	NM_023935	8064601	11	3.206	$2.30e^{-03}$	4.249	$1.70e^{-04}$
IRF8	Interferon regulatory factor 8	NM_002163	7997712	11	5.891	$3.90e^{-06}$	3.163	$2.60e^{-03}$
IARS	Isoleucyl-tRNA synthetase	NM_013417	8162313	38	4.012	$5.00e^{-11}$	1.888	$2.80e^{-03}$
SPTLC1	Serine palmitoyltransferase, long chain base subunit 1	NM_006415	8162294	16	2.669	$2.20e^{-03}$	2.983	$6.80e^{-04}$
LST1	Leukocyte specific transcript 1	NM_007161	8118149	8	4.695	$5.90e^{-04}$	3.896	$2.40e^{-03}$
AKR1CL2	Aldo-keto reductase family 1, member C-like 2	NM_001040177	7925904	13	4.268	$4.50e^{-05}$	2.834	$3.10e^{-03}$
PARVG[c]	Parvin, gamma	NM_022141	8073682	15	2.889	$1.30e^{-03}$	2.795	$1.90e^{-03}$
COL6A2	Collagen, type VI, alpha 2	NM_001849	8069301	30	2.069	$2.20e^{-03}$	2.184	$1.10e^{-03}$
CTSS[d]	Cathepsin S	NM_004079	7919800	14	3.283	$5.30e^{-04}$	2.753	$2.90e^{-03}$
HS6ST2	Heparan sulfate 6-O-sulfotransferase 2	NM_001077188	8175195	10	3.282	$3.00e^{-03}$	4.068	$5.00e^{-04}$
CHI3L1	Chitinase 3-like 1 (cartilage glycoprotein-39)	NM_001276	7923547	14	9.026	$5.70e^{-11}$	2.693	$3.50e^{-03}$
PSD3	Pleckstrin and Sec7 domain containing 3	NM_015310	8149555	18	2.395	$3.70e^{-03}$	4.342	$1.30e^{-06}$
TGFBR1	Transforming growth factor, beta receptor 1	NM_004612	8156826	11	4.710	$5.80e^{-05}$	2.999	$3.90e^{-03}$
PPHLN1	Periphilin 1	NM_016488	7954940	19	2.470	$2.20e^{-03}$	2.426	$2.10e^{-03}$
MS4A7	Membrane-spanning 4-domains, subfamily A, member 7	NM_021201	7940259	19	3.330	$5.30e^{-05}$	2.304	$4.40e^{-03}$
FAM118A	Family with sequence similarity 118, member A/B	NM_001104595	8073752	13	2.812	$3.30e^{-03}$	3.165	$1.20e^{-03}$
ITGAV	Integrin, alpha V (vitronectin receptor, alpha polypeptide	NM_002210	8046861	33	1.917	$4.00e^{-03}$	2.085	$1.30e^{-03}$
ERBB4	V-erb-a erythroblastic leukemia viral oncogene homolog 4	NM_005235	8058627	30	2.049	$2.50e^{-03}$	2.027	$2.90e^{-03}$
ZC3H14	Zinc finger CCCH-type containing 14	NM_024824	7976101	24	3.043	$3.00e^{-05}$	2.064	$5.60e^{-03}$
SYK	Spleen tyrosine kinase	NM_003177	8156321	15	2.628	$3.30e^{-03}$	2.680	$2.80e^{-03}$
RRP1B	Ribosomal RNA processing 1 homolog B (*S. cerevisiae*)	NM_015056	8068902	16	2.656	$2.30e^{-03}$	2.514	$3.80e^{-03}$

Gene Symbol	Gene Product	Reference Sequence	Transcript Cluster ID	Probe Sets (*n*)	BA10		CAUD	
					F	*p**	*F*	*p**
SLC6A18	Solute carrier family 6, member 18	NM_182632	8104281	16	2.565	$3.10e^{-03}$	2.581	$3.00e^{-03}$
CIT	Citron (rho-interacting, serine)	NM_007174	7966878	50	1.649	$6.60e^{-03}$	3.008	$4.60e^{-09}$
C3	Complement component 3	NM_000064	8033257	42	2.629	$2.50e^{-06}$	1.720	$6.70e^{-03}$
SIK1	Salt-inducible kinase 1	NM_173354	8070665	15	2.408	$7.00e^{-03}$	3.524	$1.50e^{-04}$
UHRF2	Ubiquitin-like with PHD and ring finger domains 2	NM_152896	8154316	16	4.970	$5.60e^{-07}$	2.323	$7.60e^{-03}$
FCGBP	Fc fragment of IgG binding protein	NM_003890	8036787	20	2.370	$2.70e^{-03}$	2.229	$5.00e^{-03}$
CRHR1	Corticotropin releasing hormone receptor 1	NM_001145146	8007808	17	2.730	$1.30e^{-03}$	2.312	$6.40e^{-03}$
ALDOA	Aldolase A, fructose-bisphosphate	NM_000034	7994737	18	2.354	$4.40e^{-03}$	2.418	$3.40e^{-03}$
ATP5SL	ATP5S-like	NM_018035	8037037	5	4.702	$6.00e^{-03}$	5.856	$2.00e^{-03}$
MCM6	Minichromosome maintenance complex component 6	NM_005915	8055426	18	3.304	$9.00e^{-05}$	2.206	$7.90e^{-03}$
ENTPD1	Ectonucleoside triphosphate diphosphohydrolase 1	NM_001776	7929511	13	2.696	$4.70e^{-03}$	2.793	$3.50e^{-03}$
NCF4	Neutrophil cytosolic factor 4, 40kDa	NM_013416	8072744	12	3.347	$1.00e^{-03}$	2.649	$7.20e^{-03}$
ERCC8	Excision repair cross-complementing rodent repair deficiency	NM_000082	8112285	16	3.321	$2.00e^{-04}$	2.305	$8.00e^{-03}$
HNRNPAB	Heterogeneous nuclear ribonucleoprotein A	NM_031266	8110450	10	2.958	$6.30e^{-03}$	3.404	$2.20e^{-03}$
SLC30A10	Solute carrier family 30, member 10	NM_018713	7924342	8	3.763	$3.00e^{-03}$	3.388	$5.90e^{-03}$
FYB	FYN binding protein (FYB-120)	NM_001465	8111739	17	2.763	$1.10e^{-03}$	2.260	$7.80e^{-03}$
SCAMP2	Secretory carrier membrane protein 2	NM_005697	7990417	11	4.307	$1.50e^{-04}$	2.682	$8.80e^{-03}$
TYROBP	TYRO protein tyrosine kinase binding protein	NM_003332	8036224	7	5.079	$7.30e^{-04}$	3.458	$8.40e^{-03}$
PDIA2	Protein disulfide isomerase family A, member 2	NM_006849	7991815	12	3.062	$2.30e^{-03}$	2.662	$6.90e^{-03}$
ARPC1B	Actin related protein 2	NM_005720	8134552	11	2.669	$9.10e^{-03}$	4.392	$1.00e^{-04}$
CD68	CD68 molecule	NM_001251	8004510	10	5.239	$4.10e^{-05}$	2.791	$9.20e^{-03}$
H2AFJ[e]	H2A histone family, member J	NM_177925	7954124	7	3.541	$7.40e^{-03}$	4.369	$2.10e^{-03}$
SECISBP2L	SECIS binding protein 2-like	NM_014701	7988581	19	2.197	$6.90e^{-03}$	2.415	$2.70e^{-03}$
RNF7	Ring finger protein 7	NM_014245	8083119	9	3.456	$3.20e^{-03}$	3.107	$6.60e^{-03}$
BIRC6	Baculoviral IAP repeat-containing 6	NM_016252	8041283	76	1.561	$3.50e^{-03}$	1.510	$6.30e^{-03}$
RTKN2	Rhotekin 2	NM_145307	7933855	16	2.650	$2.30e^{-03}$	2.314	$7.80e^{-03}$
IL13RA1[b]	Interleukin 13 receptor, alpha 1	NM_001560	8169580	17	2.254	$8.00e^{-03}$	2.570	$2.40e^{-03}$
C1QC	Complement component 1, q subcomponent, C chain	NM_001114101	7898799	5	13.897	$5.30e^{-06}$	4.158	$1.07e^{-02}$

Gene Symbol	Gene Product	Reference Sequence	Transcript Cluster ID	Probe Sets (*n*)	BA10		CAUD	
					F	*p**	*F*	*p**
BTF3	Basic transcription factor 3	NM_001037637	8106181	7	3.305	$1.08e^{-02}$	6.077	$1.80e^{-04}$
WDR74	WD repeat domain 74	NM_018093	7948881	12	3.360	$1.00e^{-03}$	2.525	$1.01e^{-02}$
CD37	CD37 molecule	NM_001774	8030277	14	3.460	$3.00e^{-04}$	2.340	$1.09e^{-02}$
OSBP	Oxysterol binding protein	NM_002556	7948379	17	2.940	$5.70e^{-04}$	2.174	$1.07e^{-02}$
AVPR2	Arginine vasopressin receptor 2	NM_001146151	8170794	8	3.072	$1.05e^{-02}$	4.186	$1.40e^{-03}$
SAFB2	Scaffold attachment factor B2	NM_014649	8032974	21	2.003	$1.15e^{-02}$	2.652	$5.70e^{-04}$
SYNPO	Synaptopodin	NM_007286	8109305	9	2.907	$1.00e^{-02}$	3.661	$2.10e^{-03}$
TCIRG1	T-cell, immune regulator 1, ATPase, H^+ transporting	NM_006019	7941985	21	2.165	$5.60e^{-03}$	2.111	$7.10e^{-03}$
RPS28	Ribosomal protein S28	NM_001031	8025395	6	3.525	$1.26e^{-02}$	7.811	$8.30e^{-05}$
LGALS9C	Lectin, galactoside-binding, soluble, 9C	NM_001040078	8005458	12	6.102	$8.60e^{-07}$	2.430	$1.31e^{-02}$
CDC42BPA	CDC42 binding protein kinase alpha (DMPK-like)	NM_003607	7924773	43	2.006	$5.80e^{-04}$	1.627	$1.27e^{-02}$
NUDT9	Nudix (nucleoside diphosphate linked moiety X)-type motif	NM_024047	8096251	13	3.337	$6.90e^{-04}$	2.361	$1.27e^{-02}$
CYBB	Cytochrome b-245, beta polypeptide	NM_000397	8166730	14	3.664	$1.60e^{-04}$	2.272	$1.35e^{-02}$
FGR	Gardner-Rasheed feline sarcoma viral (v-fgr) oncogene homolog	NM_005248	7914112	14	2.645	$4.10e^{-03}$	2.380	$9.60e^{-03}$
GNPTAB	N-acetylglucosamine-1-phosphate transferase, alpha and beta	NM_024312	7965812	23	1.920	$1.30e^{-02}$	2.478	$8.10e^{-04}$
ELK1	ELK1, member of ETS oncogene family	NM_001114123	8172345	12	3.579	$5.50e^{-04}$	2.425	$1.33e^{-02}$
RGPD1	RANBP2-like and GRIP domain containing 1	NM_001024457	8053622	23	3.369	$7.80e^{-06}$	1.902	$1.41e^{-02}$
CYTL1	Cytokine-like 1	NM_018659	8099132	7	3.145	$1.39e^{-02}$	5.361	$4.90e^{-04}$
LGALS9B	Lectin, galactoside-binding, soluble, 9B	NM_001042685	8013450	14	4.636	$7.60e^{-06}$	2.249	$1.45e^{-02}$
BSG	Basigin (Ok blood group)	NM_001728	8023955	12	2.420	$1.35e^{-02}$	3.196	$1.60e^{-03}$
PPP2R5B	Protein phosphatase 2, regulatory subunit B′, beta isoform	NM_006244	7941087	16	2.124	$1.53e^{-02}$	3.889	$2.50e^{-05}$
NR1D2	Nuclear receptor subfamily 1, group D, member 2	NM_005126	8078272	11	2.640	$9.80e^{-03}$	2.856	$5.70e^{-03}$
ITGB2	Integrin, beta 2 (complement component 3 receptor 3 and 4)	NM_000211	8070826	20	3.943	$2.10e^{-06}$	1.962	$1.58e^{-02}$
BEX4	Brain expressed, X-linked 4	NM_001080425	8169009	5	5.476	$2.80e^{-03}$	3.973	$1.30e^{-02}$
SERPINA1	Serpin peptidase inhibitor, clade A (alpha-1)	NM_001002236	7981068	9	6.057	$2.20e^{-05}$	2.684	$1.60e^{-02}$
ALOX5	Arachidonate 5-lipoxygenase	NM_000698	7927215	15	7.011	$2.60e^{-09}$	2.161	$1.60e^{-02}$
MORC2	MORC family CW-type zinc finger 2	NM_014941	8075430	27	2.332	$7.60e^{-04}$	1.798	$1.54e^{-02}$
PASK	PAS domain containing serine	NM_015148	8060205	19	2.946	$2.80e^{-04}$	1.988	$1.62e^{-02}$

Gene Symbol	Gene Product	Reference Sequence	Transcript Cluster ID	Probe Sets (*n*)	BA10		CAUD	
					F	*p**	*F*	*p**
IFNGR1[b]	Interferon gamma receptor 1	NM_000416	8129861	10	2.933	$7.00e^{-03}$	2.756	$1.00e^{-02}$
ACTN1[a,c]	Actinin, alpha 1	NM_001130004	7979824	24	1.978	$9.00e^{-03}$	1.987	$8.20e^{-03}$
FAM50B	Family with sequence similarity 50, member B	NM_012135	8116658	3	6.831	$1.00e^{-02}$	7.868	$6.60e^{-03}$
LPAR5	Lysophosphatidic acid receptor 5	NM_020400	7960637	4	5.092	$1.00e^{-02}$	5.541	$7.10e^{-03}$
LIPA	Lipase A, lysosomal acid, cholesterol esterase	NM_001127605	7934920	15	2.567	$4.00e^{-03}$	2.216	$1.34e^{-02}$
SAMHD1	SAM domain and HD domain 1	NM_015474	8066117	18	8.354	$7.60e^{-13}$	2.002	$1.76e^{-02}$
CD53	CD53 molecule	NM_000560	7903893	12	2.329	$1.70e^{-02}$	3.636	$4.70e^{-04}$
DDX5	DEAD (Asp-Glu-Ala-Asp) box polypeptide 5	NM_004396	8017634	16	2.088	$1.70e^{-02}$	3.002	$6.40e^{-04}$
DCLK1	Doublecortin-like kinase 1	NM_004734	7970954	18	2.446	$3.00e^{-03}$	2.044	$1.50e^{-02}$
EPRS	Glutamyl-prolyl-tRNA synthetase	NM_004446	7924351	34	1.661	$1.90e^{-02}$	3.021	$1.00e^{-06}$
HSPA4	Heat shock 70kDa protein 4	NM_002154	8108015	24	1.819	$1.87e^{-02}$	3.849	$3.70e^{-07}$
GSTM1	Glutathione S-transferase mu 1	NM_000561	7903765	9	2.603	$1.89e^{-02}$	6.225	$1.70e^{-05}$
S100A11	S100 calcium binding protein A11	NM_005620	7920128	6	4.134	$5.60e^{-03}$	3.481	$1.34e^{-02}$
ARHGAP26	Rho GTPase activating protein 26	NM_015071	8108873	26	2.376	$7.20e^{-04}$	1.781	$1.86e^{-02}$
BAIAP3	BAI1-associated protein 3	NM_003933	7992219	35	1.655	$1.81e^{-02}$	2.040	$1.30e^{-03}$
FAM111B	Family with sequence similarity 111, member B	NM_198947	7940147	5	4.244	$9.70e^{-03}$	4.211	$1.01e^{-02}$
LGMN	Legumain	NM_005606	7980958	11	4.797	$4.70e^{-05}$	2.357	$2.01e^{-02}$
CSF2RA[b]	Colony stimulating factor 2 receptor, alpha, low-affinity	NM_001161531	8165735	16	2.081	$1.80e^{-02}$	2.636	$2.40e^{-03}$
CSF2RA[b]	Colony stimulating factor 2 receptor, alpha, low-affinity	NM_001161531	8176306	16	2.081	$1.80e^{-02}$	2.636	$2.40e^{-03}$
KDM5B	Lysine (K)-specific demethylase 5B	NM_006618	7923453	29	1.851	$9.00e^{-03}$	1.821	$1.11e^{-02}$
PPP2R2A	Protein phosphatase 2 (formerly 2A), regulatory subunit	NM_002717	8145440	13	2.204	$2.00e^{-02}$	3.410	$5.60e^{-04}$
UTRN[a,c]	Utrophin	NM_007124	8122464	72	1.415	$2.10e^{-02}$	4.946	$7.10e^{-26}$
BAX	BCL2-associated X protein	NR_027882	8030158	12	2.659	$7.00e^{-03}$	2.410	$1.39e^{-02}$
MUM1	Melanoma associated antigen (mutated) 1	NR_024247	8024255	17	4.409	$2.00e^{-06}$	1.986	$2.15e^{-02}$
ZNF509	Zinc finger protein 509	NM_145291	8093829	9	2.619	$1.83e^{-02}$	3.417	$3.50e^{-03}$
GABARAPL2	GABA(A) receptor-associated protein-like 2	NM_007285	7997272	8	2.694	$2.12e^{-02}$	4.776	$5.10e^{-04}$
CHST15	Carbohydrate (N-acetylgalactosamine 4-sulfate 6-O)	NM_015892	7936856	14	2.139	$2.05e^{-02}$	3.019	$1.20e^{-03}$

Gene Symbol	Gene Product	Reference Sequence	Transcript Cluster ID	Probe Sets (*n*)	BA10		CAUD	
					F	*p**	*F*	*p**
CD247	CD247 molecule	NM_198053	7922040	10	3.484	$1.90e^{-03}$	2.457	$2.00e^{-02}$
SBF2	SET binding factor 2	NM_030962	7946516	42	1.740	$5.80e^{-03}$	1.599	$1.66e^{-02}$
SEC13	SEC13 homolog (*S. cerevisiae*)	NR_024272	8085300	10	3.295	$2.90e^{-03}$	2.465	$1.96e^{-02}$
PWP2	PWP2 periodic tryptophan protein homolog (yeast)	NM_005049	8069003	22	1.965	$1.19e^{-02}$	1.986	$1.08e^{-02}$
ELMOD3	ELMO/CED-12 domain containing 3	NM_001135021	8043131	21	2.138	$6.30e^{-03}$	1.920	$1.66e^{-02}$
ZFP82	Zinc finger protein 82 homolog (mouse)	NM_133466	8036309	8	2.874	$1.52e^{-02}$	3.222	$8.00e^{-03}$
APBB1IP	Amyloid beta (A4) precursor protein-binding, family B, m	NM_019043	7926786	18	1.969	$2.00e^{-02}$	2.374	$4.10e^{-03}$
IGSF6	Immunoglobulin superfamily, member 6	NM_005849	8000184	7	9.837	$2.00e^{-06}$	2.800	$2.44e^{-02}$
HDDC2	HD domain containing 2	NM_016063	8129363	11	2.423	$1.70e^{-02}$	2.736	$7.70e^{-03}$
GRK1	G protein-coupled receptor kinase 1	NM_002929	7970325	3	12.093	$1.30e^{-03}$	5.219	$2.34e^{-02}$
C6orf114	Chromosome 6 open reading frame 114	AF264036	8123981	3	8.242	$5.60e^{-03}$	5.597	$1.92e^{-02}$
PEX10	Peroxisomal biogenesis factor 10	NM_153818	7911720	9	2.496	$2.37e^{-02}$	3.854	$1.40e^{-03}$
RBM12B	RNA binding motif protein 12B	NM_203390	8151788	6	3.592	$1.15e^{-02}$	3.472	$1.36e^{-02}$
TRPM3	Transient receptor potential cation channel, subfamily M	NM_206946	8161654	38	1.574	$2.51e^{-02}$	2.281	$1.30e^{-04}$
PHKG2	Phosphorylase kinase, gamma 2 (testis)	NM_000294	7994928	10	2.654	$1.27e^{-02}$	2.651	$1.27e^{-02}$
C20orf11	Chromosome 20 open reading frame 11	NM_017896	8064007	6	4.198	$5.20e^{-03}$	3.173	$2.04e^{-02}$
GFM2	G elongation factor, mitochondrial 2	NM_032380	8112622	23	1.770	$2.61e^{-02}$	2.695	$2.70e^{-04}$
RUNX1T1	Runt-related transcription factor 1; translocated to, 1	NM_175634	8151768	15	2.030	$2.47e^{-02}$	2.813	$1.70e^{-03}$
CHAF1B	Chromatin assembly factor 1, subunit B (p60)	NM_005441	8068478	15	2.618	$3.40e^{-03}$	2.047	$2.33e^{-02}$
ZNF483	Zinc finger protein 483	NM_133464	8157193	9	2.486	$2.42e^{-02}$	3.560	$2.60e^{-03}$
C6orf25	Chromosome 6 open reading frame 25	NM_138277	8178074	5	3.752	$1.65e^{-02}$	4.142	$1.09e^{-02}$
TSPY1	Testis specific protein, Y-linked 1	NM_003308	8176524	7	5.534	$3.80e^{-04}$	2.735	$2.71e^{-02}$
ZBTB8B	Zinc finger and BTB domain containing 8B	NM_001145720	7899797	13	2.231	$1.86e^{-02}$	2.472	$9.10e^{-03}$
STXBP2	Syntaxin binding protein 2	NM_006949	8025255	22	1.776	$2.79e^{-02}$	3.902	$8.40e^{-07}$
ME3	Malic enzyme 3, NADP(+)-dependent, mitochondrial	NM_001014811	7950864	18	3.910	$7.60e^{-06}$	1.876	$2.84e^{-02}$
HECW2	HECT, C2 and WW domain containing E3 ubiquitin protein	NM_020760	8057898	30	1.869	$7.60e^{-03}$	1.694	$2.09e^{-02}$
ZNF827	Zinc finger protein 827	NM_178835	8103025	15	2.204	$1.39e^{-02}$	2.177	$1.52e^{-02}$
RPS28	Ribosomal protein S28	NM_001031	7942824	5	3.249	$2.90e^{-02}$	8.974	$1.40e^{-04}$

Gene Symbol	Gene Product	Reference Sequence	Transcript Cluster ID	Probe Sets (*n*)	BA10		CAUD	
					F	*p**	*F*	*p**
FLJ46300	FLJ46300 protein	*e*NST00000341866	7937073	5	5.286	$3.40e^{-03}$	3.345	$2.60e^{-02}$
RRAGD	Ras-related GTP binding D	NM_021244	8128123	9	2.511	$2.29e^{-02}$	3.100	$6.70e^{-03}$
BRP44	Brain protein 44	NR_026550	7922095	8	4.073	$1.70e^{-03}$	2.528	$2.90e^{-02}$
ANGEL2	Angel homolog 2 (*Drosophila*)	NM_144567	7924190	12	2.190	$2.53e^{-02}$	2.744	$5.50e^{-03}$
PRRG4	Proline rich Gla (G-carboxyglutamic acid) 4 (transmembrane)	NM_024081	7939150	7	2.888	$2.11e^{-02}$	3.344	$1.01e^{-02}$
IL1B	Interleukin 1, beta	NM_000576	8054722	8	2.764	$1.86e^{-02}$	2.955	$1.30e^{-02}$
ADAR	Adenosine deaminase, RNA-specific	NM_001111	7920531	20	1.803	$3.04e^{-02}$	2.495	$1.50e^{-03}$
SYNE2[a,c]	Spectrin repeat containing, nuclear envelope 2	NM_182914	7974920	124	1.461	$1.80e^{-03}$	1.280	$3.02e^{-02}$
CXCL16	Chemokine (C-X-C motif) ligand 16	NM_022059	8011713	10	2.254	$3.19e^{-02}$	4.472	$2.10e^{-04}$
CSF1	Colony stimulating factor 1 (macrophage)	NM_000757	7903786	16	2.060	$1.91e^{-02}$	2.168	$1.31e^{-02}$
PTPRE	Protein tyrosine phosphatase, receptor type, E	NM_006504	7931353	25	1.775	$2.10e^{-02}$	1.923	$1.13e^{-02}$
ZNF540	Zinc finger protein 540	NM_152606	8028266	8	2.510	$2.99e^{-02}$	3.854	$2.50e^{-03}$
QSOX1	Quiescin Q6 sulfhydryl oxidase 1	NM_002826	7907830	16	1.925	$3.05e^{-02}$	2.686	$2.00e^{-03}$
RYR2	Ryanodine receptor 2 (cardiac)	NM_001035	7910792	104	1.364	$1.49e^{-02}$	1.351	$1.76e^{-02}$
ABCD4	ATP-binding cassette, sub-family D (ALD), member 4	NM_005050	7980115	24	1.983	$8.40e^{-03}$	1.764	$2.44e^{-02}$
SPPL2B	Signal peptide peptidase-like 2B	NM_001077238	8024446	20	1.789	$3.22e^{-02}$	2.682	$6.60e^{-04}$
CTSD	Cathepsin D	NM_001909	7945666	11	2.184	$3.11e^{-02}$	3.281	$1.90e^{-03}$
SLC9A6	Solute carrier family 9 (sodium	NM_001042537	8170097	19	2.046	$1.28e^{-02}$	1.933	$2.02e^{-02}$
ARID1A	AT rich interactive domain 1A (SWI-like)	NM_006015	7899220	23	1.720	$3.27e^{-02}$	2.524	$6.40e^{-04}$
RAPGEF4	Rap guanine nucleotide exchange factor (GEF) 4	NM_007023	8046428	32	3.159	$7.50e^{-07}$	1.585	$3.35e^{-02}$
VAPB	VAMP (vesicle-associated membrane protein)-associated protein	NM_004738	8063620	13	2.075	$2.94e^{-02}$	2.733	$4.20e^{-03}$
SLC1A1	Solute carrier family 1 (neuronal)	NM_004170	8154135	15	1.932	$3.40e^{-02}$	4.279	$1.20e^{-05}$
CIRH1A	Cirrhosis, autosomal recessive 1A (cirhin)	NM_032830	7996891	16	2.323	$7.50e^{-03}$	1.966	$2.65e^{-02}$
NCRNA00169	Non-protein coding RNA 169	NR_026675	7993821	3	4.867	$2.83e^{-02}$	8.058	$6.00e^{-03}$
ETF1	Eukaryotic translation termination factor 1	NM_004730	8114443	11	2.412	$1.75e^{-02}$	2.416	$1.73e^{-02}$
CDH5	Cadherin 5, type 2 (vascular endothelium)	NM_001795	7996264	16	1.984	$2.50e^{-02}$	2.229	$1.05e^{-02}$
ACSL4	Acyl-CoA synthetase long-chain family member 4	NM_022977	8174474	19	2.901	$3.40e^{-04}$	1.788	$3.57e^{-02}$
LRFN2[b]	Leucine rich repeat and fibronectin type III domain	NM_020737	8119390	3	14.282	$6.70e^{-04}$	4.468	$3.55e^{-02}$

Gene Symbol	Gene Product	Reference Sequence	Transcript Cluster ID	Probe Sets (*n*)	BA10		CAUD	
					F	*p**	*F*	*p**
FLJ43315	Similar to Asparagine synthetase [glutamine-hydrolyzing]	BC057848	8077198	5	5.599	$2.50e^{-03}$	3.117	$3.37e^{-02}$
RGPD1	RANBP2-like and GRIP domain containing 1	NM_001024457	8043324	22	1.747	$3.18e^{-02}$	2.158	$4.80e^{-03}$
CPSF3	Cleavage and polyadenylation specific factor 3, 73kDa	NM_016207	8040142	20	1.789	$3.21e^{-02}$	2.242	$4.70e^{-03}$
B4GALT1	UDP-Gal:betaGlcNAc beta 1,4- galactosyltransferase, poly	NM_001497	8160637	9	3.330	$4.20e^{-03}$	2.336	$3.31e^{-02}$
NPTXR	Neuronal pentraxin receptor	NM_014293	8076169	6	3.733	$9.60e^{-03}$	2.941	$2.82e^{-02}$
CYFIP1	Cytoplasmic FMR1 interacting protein 1	NM_014608	7981824	34	2.359	$1.50e^{-04}$	1.542	$3.82e^{-02}$
C9orf78	Chromosome 9 open reading frame 78	NM_016520	8164596	10	2.619	$1.40e^{-02}$	2.362	$2.49e^{-02}$
KLHL7	Kelch-like 7 (*Drosophila*)	NM_018846	8131815	15	1.979	$2.90e^{-02}$	2.319	$9.40e^{-03}$
OCRL	Oculocerebrorenal syndrome of Lowe	NM_000276	8169811	24	1.664	$3.90e^{-02}$	2.881	$7.30e^{-05}$
KPNA2	Karyopherin alpha 2 (RAG cohort 1, importin alpha 1)	NM_002266	8019737	13	2.241	$1.80e^{-02}$	2.193	$2.08e^{-02}$
RPGR	Retinitis pigmentosa GTPase regulator	NM_000328	8172056	25	1.648	$3.90e^{-02}$	2.646	$2.00e^{-04}$
ABAT	4-aminobutyrate aminotransferase	NM_020686	7993126	19	1.988	$1.60e^{-02}$	1.900	$2.30e^{-02}$
ZNF852	Zinc finger protein 852	AK296954	8086494	3	6.607	$1.20e^{-02}$	4.900	$2.78e^{-02}$
KIAA1324L	KIAA1324-like	NM_001142749	8140709	20	2.502	$1.00e^{-03}$	1.747	$3.81e^{-02}$
ATP4A	ATPase, H^+	NM_000704	8036110	22	2.147	$5.00e^{-03}$	1.727	$3.46e^{-02}$
JAKMIP2	Janus kinase and microtubule interacting protein 2	NM_014790	8114938	25	1.651	$3.80e^{-02}$	2.268	$1.60e^{-03}$
PRG2	Plasticity-related gene 2	NM_024888	8032094	11	2.426	$1.70e^{-02}$	2.305	$2.29e^{-02}$
ZMYND8	Zinc finger, MYND-type containing 8	NM_183047	8066786	31	3.091	$1.80e^{-06}$	1.565	$3.98e^{-02}$
FCGR1B	Fc fragment of IgG, high affinity Ib, receptor (CD64)	NM_001017986	7919133	5	15.021	$2.80e^{-06}$	2.970	$3.99e^{-02}$
PTBP2	Polypyrimidine tract binding protein 2	NM_021190	7903188	14	3.029	$1.20e^{-03}$	1.931	$3.88e^{-02}$
PAF1	Paf1, RNA polymerase II associated factor, homolog (*S. cerevisiae*)	NM_019088	8036720	16	3.231	$2.80e^{-04}$	1.847	$3.98e^{-02}$
CCDC90B	Coiled-coil domain containing 90B	NM_021825	7950753	8	2.743	$1.90e^{-02}$	2.700	$2.10e^{-02}$
TSPY1	Testis specific protein, Y-linked 1	NM_003308	8176508	8	3.347	$6.00e^{-03}$	2.437	$3.43e^{-02}$
CTSZ[d]	Cathepsin Z	NM_001336	8067279	8	2.353	$4.00e^{-02}$	4.688	$5.90e^{-04}$
ZDHHC16	Zinc finger, DHHC-type containing 16	NM_198046	7929634	14	2.485	$7.00e^{-03}$	1.975	$3.41e^{-02}$
SMA5	Glucuronidase, beta pseudogene	AK289851	8177544	9	2.797	$1.30e^{-02}$	2.410	$2.83e^{-02}$
CTPS	CTP synthase	NM_001905	7900510	20	1.815	$2.90e^{-02}$	2.020	$1.23e^{-02}$

Gene Symbol	Gene Product	Reference Sequence	Transcript Cluster ID	Probe Sets (*n*)	BA10		CAUD	
					F	*p**	*F*	*p**
TUBB4Q	Tubulin, beta polypeptide 4, member Q	NM_020040	8021919	4	4.782	$1.30e^{-02}$	3.797	$2.86e^{-02}$
ANXA6	Annexin A6	NM_001155	8115234	26	2.174	$2.00e^{-03}$	1.630	$3.93e^{-02}$
SMARCA1	SWI/SNF related, matrix associated, actin dependent	NM_003069	8174985	30	2.980	$5.40e^{-06}$	1.568	$4.15e^{-02}$
TMCO3	Transmembrane and coiled-coil domains 3	NM_017905	7970301	15	2.377	$7.70e^{-03}$	1.934	$3.38e^{-02}$
ULK4	Unc-51-like kinase 4 (*C. elegans*)	NM_017886	8086352	15	2.540	$4.40e^{-03}$	1.899	$3.77e^{-02}$
ZNF341	Zinc finger protein 341	NM_032819	8061946	11	4.044	$2.90e^{-04}$	2.061	$4.22e^{-02}$
TSPAN7	Tetraspanin 7	NM_004615	8166784	10	2.134	$4.21e^{-02}$	3.962	$6.40e^{-04}$
TPD52L1	Tumor protein D52-like 1	NM_001003395	8121838	11	3.000	$3.90e^{-03}$	2.091	$3.92e^{-02}$
ATP6V0E1	ATPase, H+ transporting, lysosomal 9kDa, V0 subunit e1	NM_003945	8110022	9	2.487	$2.41e^{-02}$	2.588	$1.95e^{-02}$
SREBF1	Sterol regulatory element binding transcription factor	NM_001005291	8013135	21	1.784	$2.97e^{-02}$	1.958	$1.41e^{-02}$
AQP1	Aquaporin 1 (Colton blood group)	NM_198098	8132118	11	2.545	$1.25e^{-02}$	2.176	$3.17e^{-02}$
DPY19L4	Dpy-19-like 4 (*C. elegans*)	NM_181787	8147375	20	1.731	$4.06e^{-02}$	2.306	$3.60e^{-03}$
ZWINT	ZW10 interactor	NM_032997	7933707	15	2.432	$6.40e^{-03}$	1.895	$3.83e^{-02}$
C3orf1	Chromosome 3 open reading frame 1	NM_016589	8081867	10	2.802	$9.00e^{-03}$	2.203	$3.59e^{-02}$
CCR10	Chemokine (C-C motif) receptor 10	NM_016602	8015681	3	6.185	$1.43e^{-02}$	4.721	$3.07e^{-02}$
ITGA8	Integrin, alpha 8	NM_003638	7932254	30	1.599	$3.52e^{-02}$	1.823	$9.90e^{-03}$
BRD7	Bromodomain containing 7	NM_013263	8001350	20	1.704	$4.52e^{-02}$	3.622	$9.10e^{-06}$
MPHOSPH9	M-phase phosphoprotein 9	NM_022782	7967386	25	2.763	$1.00e^{-04}$	1.615	$4.52e^{-02}$
MKLN1	Muskelin 1, intracellular mediator containing kelch motifs	NM_013255	8136259	21	1.724	$3.83e^{-02}$	2.112	$7.10e^{-03}$
UGGT1	UDP-glucose glycoprotein glucosyltransferase 1	NM_020120	8045090	43	1.496	$3.27e^{-02}$	1.617	$1.36e^{-02}$
ZCCHC2	Zinc finger, CCHC domain containing 2	NM_017742	8021546	16	2.057	$1.93e^{-02}$	1.961	$2.70e^{-02}$
STK19	Serine/threonine kinase 19	NR_026717	8118395	12	5.450	$4.20e^{-06}$	1.965	$4.64e^{-02}$
STK19	Serine/threonine kinase 19	NR_026717	8178164	12	5.450	$4.20e^{-06}$	1.965	$4.64e^{-02}$
CEMP1	Cementum protein 1	NM_001048212	7998817	2	11.348	$1.51e^{-02}$	7.819	$3.13e^{-02}$
TRPC4	Transient receptor potential cation channel, subfamily C,	NM_016179	7971104	17	1.854	$3.46e^{-02}$	2.148	$1.18e^{-02}$
PLA1A	Phospholipase A1 member A	NM_015900	8081890	12	2.641	$7.30e^{-03}$	2.029	$3.91e^{-02}$
PTGS1	Prostaglandin-endoperoxide synthase 1 (prostaglandin G	NM_000962	8157650	17	1.773	$4.61e^{-02}$	2.951	$5.40e^{-04}$
POLM	Polymerase (DNA directed), mu	NM_013284	8139281	17	1.960	$2.36e^{-02}$	1.966	$2.32e^{-02}$

Gene Symbol	Gene Product	Reference Sequence	Transcript Cluster ID	Probe Sets (*n*)	BA10		CAUD	
					F	*p**	*F*	*p**
PPM1D	Protein phosphatase 1D magnesium-dependent, delta isoform	NM_003620	8008922	10	2.872	$7.60e^{-03}$	2.164	$3.93e^{-02}$
COBLL1	COBL-like 1	NM_014900	8056343	15	2.081	$2.09e^{-02}$	2.014	$2.61e^{-02}$
CTSL2[d]	Cathepsin L2	NM_001333	8162652	11	2.613	$1.05e^{-02}$	2.119	$3.66e^{-02}$
TRIM22	Tripartite motif-containing 22	NM_006074	7938035	11	2.867	$5.50e^{-03}$	2.063	$4.20e^{-02}$
FLII	Flightless I homolog (*Drosophila*)	NM_002018	8013191	30	2.052	$2.50e^{-03}$	1.552	$4.53e^{-02}$
EEF1A2	Eukaryotic translation elongation factor 1 alpha 2	NM_001958	8067652	9	2.183	$4.55e^{-02}$	3.504	$2.90e^{-03}$
AGFG1	ArfGAP with FG repeats 1	NM_001135187	8048847	16	1.791	$4.80e^{-02}$	2.931	$8.20e^{-04}$
GMDS	GDP-mannose 4,6-dehydratase	NM_001500	8123562	16	1.804	$4.60e^{-02}$	2.597	$2.80e^{-03}$
TMC3	Transmembrane channel-like 3	NM_001080532	7990848	24	1.660	$3.94e^{-02}$	1.987	$9.40e^{-03}$
USP18	Ubiquitin specific peptidase 18	NM_017414	8071155	5	2.875	$4.45e^{-02}$	5.041	$4.30e^{-03}$
PTPRS[b]	Protein tyrosine phosphatase, receptor type, S	NM_002850	8032926	38	2.614	$8.10e^{-06}$	1.469	$4.89e^{-02}$
ATP13A2	ATPase type 13A2	NM_022089	7912898	29	1.745	$1.71e^{-02}$	1.630	$3.19e^{-02}$
ARX	Aristaless related homeobox	NM_139058	8171867	6	2.693	$3.99e^{-02}$	3.754	$9.30e^{-03}$
AP2A1	Adaptor-related protein complex 2, alpha 1 subunit	NM_014203	8030470	27	2.989	$1.40e^{-05}$	1.569	$4.95e^{-02}$
LAT	Linker for activation of T cells	NM_014387	7994541	17	2.383	$4.90e^{-03}$	1.782	$4.47e^{-02}$
PLVAP	Plasmalemma vesicle associated protein	NM_031310	8035297	6	2.663	$4.16e^{-02}$	3.832	$8.40e^{-03}$
SLC25A46	Solute carrier family 25, member 46	NM_138773	8107259	10	2.503	$1.80e^{-02}$	2.251	$3.21e^{-02}$
DPF1	D4, zinc and double PHD fingers family 1	NM_004647	8036460	12	1.949	$4.85e^{-02}$	3.183	$1.60e^{-03}$
PDGFD	Platelet derived growth factor D	NM_025208	7951351	11	2.718	$8.00e^{-03}$	2.057	$4.27e^{-02}$
C1orf175	Chromosome 1 open reading frame 175	NR_026782	7901634	27	1.727	$2.23e^{-02}$	1.680	$2.85e^{-02}$
POM121	POM121 membrane glycoprotein (rat)	NM_172020	8133275	17	1.804	$4.14e^{-02}$	2.204	$9.60e^{-03}$
SUGT1	SGT1, suppressor of G2 allele of SKP1 (*S. cerevisiae*)	NM_001130912	7969271	14	2.474	$7.10e^{-03}$	1.891	$4.39e^{-02}$
TSPY1	Testis specific protein, Y-linked 1	NM_003308	8176544	8	2.657	$2.28e^{-02}$	2.537	$2.85e^{-02}$
TBC1D21	TBC1 domain family, member 21	NM_153356	7984759	11	2.383	$1.88e^{-02}$	2.164	$3.26e^{-02}$
CMTM4	CKLF-like MARVEL transmembrane domain containing 4	NM_181521	8001830	10	2.095	$4.60e^{-02}$	3.016	$5.50e^{-03}$
LST1	Leukocyte specific transcript 1	NM_007161	8177988	7	2.367	$4.97e^{-02}$	4.478	$1.70e^{-03}$
LST1	Leukocyte specific transcript 1	NM_007161	8179268	7	2.367	$4.97e^{-02}$	4.478	$1.70e^{-03}$
OAS2	2′-5′-oligoadenylate synthetase 2, 69/71 kDa	NM_002535	7958913	17	1.759	$4.84e^{-02}$	2.399	$4.60e^{-03}$

Schizophr Res. Author manuscript; available in PMC 2013 December 01.

Gene Symbol	Gene Product	Reference Sequence	Transcript Cluster ID	Probe Sets (*n*)	BA10		CAUD	
					F	*p**	*F*	*p**
TNS1	Tensin 1	NM_022648	8058869	35	1.578	$2.92e^{-02}$	1.609	$2.41e^{-02}$
ECSIT	ECSIT homolog (*Drosophila*)	NM_016581	8034286	10	2.653	$1.27e^{-02}$	2.146	$4.09e^{-02}$
PCMTD1	Protein-L-isoaspartate (D-aspartate) O-methyltransferase	NM_052937	8150714	7	2.696	$2.89e^{-02}$	2.785	$2.50e^{-02}$
RBAK	RB-associated KRAB zinc finger	NM_021163	8131292	3	5.417	$2.11e^{-02}$	4.573	$3.34e^{-02}$
RBM33	RNA binding motif protein 33	NM_053043	8137542	15	2.154	$1.64e^{-02}$	1.896	$3.82e^{-02}$
GCN1L1	GCN1 general control of amino-acid synthesis 1-like 1	NM_006836	7966938	57	1.620	$5.50e^{-03}$	1.372	$4.91e^{-02}$
SSH2	Slingshot homolog 2 (*Drosophila*)	NM_033389	8013965	19	2.277	$4.90e^{-03}$	1.702	$4.97e^{-02}$
ZPLD1	Zona pellucida-like domain containing 1	NM_175056	8081407	19	1.806	$3.33e^{-02}$	1.919	$2.13e^{-02}$
CKS2	CDC28 protein kinase regulatory subunit 2	NM_001827	8156290	4	3.169	$4.96e^{-02}$	5.916	$5.40e^{-03}$
EGFLAM[b]	EGF-like, fibronectin type III and laminin G domains	NM_152403	8105013	26	1.853	$1.28e^{-02}$	1.614	$4.25e^{-02}$
UROD	Uroporphyrinogen decarboxylase	NM_000374	7901073	13	2.013	$3.52e^{-02}$	2.202	$2.03e^{-02}$
CWH43	Cell wall biogenesis 43 C-terminal homolog (*S. cerevisiae*)	AK300495	8095005	3	4.689	$3.13e^{-02}$	5.063	$2.55e^{-02}$
REL	V-rel reticuloendotheliosis viral oncogene homolog (avian)	NM_002908	8042144	12	1.948	$4.86e^{-02}$	2.579	$8.70e^{-03}$
EPB41	Erythrocyte membrane protein band 4.1 (elliptocytosis 1, R)	NM_203342	7899534	25	1.605	$4.73e^{-02}$	1.914	$1.05e^{-02}$
TSPY1	Testis specific protein, Y-linked 1	NM_003308	8176484	9	2.411	$2.83e^{-02}$	2.383	$3.00e^{-02}$
TM2D2	TM2 domain containing 2	NM_031940	8150364	8	2.444	$3.39e^{-02}$	2.620	$2.44e^{-02}$
CLSPN	Claspin homolog (*Xenopus laevis*)	NM_022111	7914851	26	1.691	$2.92e^{-02}$	1.690	$2.93e^{-02}$
CKMT1A	Creatine kinase, mitochondrial 1A	NM_001015001	7983256	13	1.890	$4.98e^{-02}$	2.488	$8.70e^{-03}$
THADA	Thyroid adenoma associated	NM_022065	8051820	41	1.652	$1.21e^{-02}$	1.455	$4.68e^{-02}$
GPR179	G protein-coupled receptor 179	NM_001004334	8014666	12	2.309	$1.83e^{-02}$	2.014	$4.07e^{-02}$
PNPLA8	Patatin-like phospholipase domain containing 8	NM_015723	8142307	16	1.784	$4.92e^{-02}$	2.237	$1.03e^{-02}$
IGDCC3[b]	Immunoglobulin superfamily, DCC subclass, member 3	NM_004884	7989770	14	2.267	$1.37e^{-02}$	1.877	$4.58e^{-02}$
ADAM9	ADAM metallopeptidase domain 9 (meltrin gamma)	NM_003816	8146000	23	1.714	$3.35e^{-02}$	1.769	$2.61e^{-02}$
PNKP	Polynucleotide kinase 3′-phosphatase	NM_007254	8038458	18	1.813	$3.60e^{-02}$	1.924	$2.38e^{-02}$
IFITM2	Interferon induced transmembrane protein 2 (1–8D)	NM_006435	7937330	4	3.691	$3.13e^{-02}$	3.793	$2.87e^{-02}$
KCNG2	Potassium voltage-gated channel, subfamily G, member 2	NM_012283	8021900	2	8.880	$2.46e^{-02}$	7.247	$3.60e^{-02}$
LHFPL2	Lipoma HMGIC fusion partner-like 2	NM_005779	8112803	3	4.391	$3.71e^{-02}$	5.200	$2.36e^{-02}$
PDCD11	Programmed cell death 11	NM_014976	7930226	37	1.615	$2.04e^{-02}$	1.503	$4.15e^{-02}$

Gene Symbol	Gene Product	Reference Sequence	Transcript Cluster ID	Probe Sets (*n*)	BA10		CAUD	
					F	*p**	*F*	*p**
HIST1H4H[e]	Histone cluster 1, H4h	NM_003543	8124448	4	4.697	$1.36e^{-02}$	3.188	$4.88e^{-02}$
SDCBP	Syndecan binding protein (syntenin)	NM_005625	8146550	8	2.390	$3.75e^{-02}$	2.603	$2.52e^{-02}$
MGC42105	Serine	NM_153361	8105146	4	3.781	$2.90e^{-02}$	3.602	$3.38e^{-02}$
DIAPH1	Diaphanous homolog 1 (*Drosophila*)	NM_005219	8114658	32	1.522	$4.75e^{-02}$	1.716	$1.56e^{-02}$
IL17RA	Interleukin 17 receptor A	NM_014339	8071069	14	2.100	$2.32e^{-02}$	1.921	$4.00e^{-02}$
MYO18A	Myosin XVIIIA	NM_078471	8013860	45	1.474	$3.49e^{-02}$	1.502	$2.85e^{-02}$
ACLY	ATP citrate lyase	NM_001096	8015460	29	1.687	$2.35e^{-02}$	1.587	$4.00e^{-02}$
KCNH3	Potassium voltage-gated channel, subfamily H (eag-related)	NM_012284	7955231	16	1.794	$4.76e^{-02}$	2.090	$1.73e^{-02}$
CAMTA2	Calmodulin binding transcription activator 2	NM_015099	8011774	22	1.642	$4.96e^{-02}$	1.908	$1.55e^{-02}$
CD4	CD4 molecule	NM_000616	7953428	13	2.282	$1.60e^{-02}$	1.896	$4.91e^{-02}$
PLXNB1	Plexin B1	NM_001130082	8086908	40	1.452	$4.98e^{-02}$	1.625	$1.57e^{-02}$
WISP1	WNT1 inducible signaling pathway protein 1	NM_003882	8148435	10	2.379	$2.39e^{-02}$	2.138	$4.17e^{-02}$
SLC18A2	Solute carrier family 18 (vesicular monoamine), member 2	NM_003054	7930837	19	1.942	$1.95e^{-02}$	1.720	$4.64e^{-02}$
KPNA2	Karyopherin alpha 2 (RAG cohort 1, importin alpha 1)	NM_002266	8009417	12	2.332	$1.72e^{-02}$	1.940	$4.96e^{-02}$
MAPRE3[c]	Microtubule-associated protein, RP	NM_012326	8040742	10	2.330	$2.68e^{-02}$	2.148	$4.07e^{-02}$
RPL9	Ribosomal protein L9	NM_001024921	8099887	9	2.281	$3.71e^{-02}$	2.346	$3.24e^{-02}$
FOXD4L6	Forkhead box D4-like 6	NM_001085476	8161533	3	4.580	$3.33e^{-02}$	4.399	$3.69e^{-02}$
TGM2[b]	Transglutaminase 2 (C polypeptide, protein-glutamine-gamma)	NM_004613	8066214	16	1.858	$3.83e^{-02}$	1.908	$3.23e^{-02}$
ZDHHC17	Zinc finger, DHHC-type containing 17	NM_015336	7957277	20	1.838	$2.63e^{-02}$	1.708	$4.46e^{-02}$
ATP9A	ATPase, class II, type 9A	NM_006045	8067055	31	1.553	$4.25e^{-02}$	1.623	$2.88e^{-02}$
ZNF382	Zinc finger protein 382	NM_032825	8028194	5	3.392	$2.46e^{-02}$	2.834	$4.67e^{-02}$
HIST1H3D[e]	Histone cluster 1, H3d	NM_003530	8124416	6	2.717	$3.86e^{-02}$	2.824	$3.32e^{-02}$
SLC25A3	Solute carrier family 25 (mitochondrial carrier)	NM_213611	7957746	12	2.217	$2.35e^{-02}$	1.946	$4.88e^{-02}$
C12orf56	Chromosome 12 open reading frame 56	NM_001099676	7964687	11	2.185	$3.10e^{-02}$	2.051	$4.32e^{-02}$
AEBP1	AE binding protein 1	NM_001129	8132557	22	1.699	$3.91e^{-02}$	1.714	$3.65e^{-02}$
TNPO1	Transportin 1	NM_002270	8106122	18	1.748	$4.58e^{-02}$	1.863	$2.99e^{-02}$
ACOT2	Acyl-CoA thioesterase 2	NM_006821	7975602	4	3.878	$2.66e^{-02}$	3.175	$4.93e^{-02}$
POLR3E	Polymerase (RNA) III (DNA directed) polypeptide E (80kDa)	NM_018119	7993973	25	1.693	$3.14e^{-02}$	1.613	$4.56e^{-02}$

Gene Symbol	Gene Product	Reference Sequence	Transcript Cluster ID	Probe Sets (*n*)	BA10		CAUD	
					F	*p**	*F*	*p**
STK32A	Serine/threonine kinase	NM_001112724	8108981	13	1.971	$3.96e^{-02}$	1.954	$4.16e^{-02}$
PARP14	Poly (ADP-ribose) polymerase family, member 14	NM_017554	8082100	17	1.864	$3.35e^{-02}$	1.755	$4.91e^{-02}$
FOLR3	Folate receptor 3 (gamma)	NM_000804	7942328	3	4.042	$4.55e^{-02}$	4.389	$3.71e^{-02}$
HIST1H2BD[e]	Histone cluster 1, H2bd	NM_021063	8117382	6	2.783	$3.51e^{-02}$	2.808	$4.82e^{-02}$
CRLF3[b]	Cytokine receptor-like factor 3	NM_015986	8014037	9	2.313	$3.47e^{-02}$	2.141	$4.97e^{-02}$
MLC1	Megalencephalic leukoencephalopathy with subcortical cysts	NM_015166	8076894	14	1.915	$4.08e^{-02}$	1.881	$4.53e^{-02}$
DNAJC9	DnaJ (Hsp40) homolog, subfamily C, member 9	NM_015190	7934320	5	2.882	$4.42e^{-02}$	2.912	$4.27e^{-02}$
MTSS1	Metastasis suppressor 1	NM_014751	8152764	17	1.780	$4.51e^{-02}$	1.799	$4.21e^{-02}$
GLRX3	Glutaredoxin 3	NM_006541	7931393	9	2.197	$4.42e^{-02}$	2.140	$4.98e^{-02}$
ACSL5	Acyl-CoA synthetase long-chain family member 5	NM_016234	7930498	25	1.610	$4.64e^{-02}$	1.602	$4.79e^{-02}$
NR4A1	Nuclear receptor subfamily 4, group A, member 1	NM_002135	7955589	16	1.787	$4.87e^{-02}$	1.785	$4.90e^{-02}$

* Rows are sorted in ascending order by the average *p*-value across both brain regions.

[a] Genes encoding proteins with actinin-type actin-binding domains

[b] Genes encoding proteins with fibronectin type-III-folds

[c] Genes encoding proteins with calponin-like actin-binding domains

[d] Genes encoding proteins with peptidase C1A, papain C-terminals

[e] Genes encoding histone core proteins